frontiers | Frontiers in Marine Science

TYPE Original Research
PUBLISHED 23 July 2024
DOI 10.3389/fmars.2024.1414673

OPEN ACCESS

EDITED BY
Wen-Cheng Wang,
National Taiwan Normal University, Taiwan

REVIEWED BY
Giovanni Martinelli,
National Institute of Geophysics and Volcanology, Italy
Cuiling Xu,
Qingdao Institute of Marine Geology (QIMG), China

*CORRESPONDENCE
Irina Marilena Stanciu
irina.stanciu@geoecomar.ro

RECEIVED 09 April 2024
ACCEPTED 25 June 2024
PUBLISHED 23 July 2024

CITATION
Popa A, Stanciu IM, Drăguşin V, Teacă A, Balan SV, Popa ME, Ion G and Ispas B-A (2024) Geophysical and geochemical investigations of underwater sulphurous seeps from Western Black Sea (Mangalia area, Romania), in support of habitat conservation. *Front. Mar. Sci.* 11:1414673. doi: 10.3389/fmars.2024.1414673

Geophysical and geochemical investigations of underwater sulphurous seeps from Western Black Sea (Mangalia area, Romania), in support of habitat conservation

Adrian Popa[1,2], Irina Marilena Stanciu[1]*, Virgil Drăguşin[3], Adrian Teacă[1], Sorin Vasile Balan[1,2], Mihai Emilian Popa[2,4], Gabriel Ion[1] and Bogdan-Adrian Ispas[1]

[1]National Institute for Research and Development for Marine Geology and Geo-Ecology - GeoEcoMar, Bucharest/Constanţa, Romania, [2]Doctoral School of Geology, Faculty of Geology and Geophysics, University of Bucharest, Bucharest, Romania, [3]Emil Racoviţă Institute of Speleology, Romanian Academy, Bucharest, Romania, [4]School of Geoscience and Technology, Southwest Petroleum University, Chengdu, China

Mangalia area harbors in the western Black Sea a distinctive marine environment thriving under specific hydrochemical conditions, largely influenced by a significant number of sulphurous springs occurring in shallow marine waters. These springs led to the designation of the area as part of the Natura 2000 Marine Protected Area (MPA) network at European level (Underwater Sulphurous Springs from Mangalia - ROSAC0094), as unique hydro-geomorphological features in the region. In 2021 and 2023, two research cruises led by GeoEcoMar investigated underwater sulphurous springs primarily located offshore of Mangalia (Constanţa County, Romania). The study area, located between 17-29 meters water depth and 1.8-3 km offshore, encompasses two marine protected areas: the Underwater Sulphurous Springs from Mangalia (ROSAC0094) and Cape Aurora (ROSCI0281). The research combined geophysical and geochemical techniques and sediment sampling. Considering the susceptibility of these natural systems to human activities such as fishing and dredging, as well as the impact of ecological and climate changes, this paper offers significant insights contributing to the development of effective conservation and management strategies for these environments. The surveys were conducted for benthic habitats mapping, with the objective of improving our understanding of these ecosystems' distribution, composition and dynamics. As these sulphurous waters are rich in methane, a powerful greenhouse gas, our results also contribute to the inventory of greenhouse gas sources. The results presented in this paper provide valuable new insights into this specific environment, contributing to the understanding of its complex functioning and evolution.

KEYWORDS

underwater sulphurous springs, habitat mapping, Mangalia area, Romania, Black Sea

1 Introduction

The Romanian Black Sea coastline stretches over 244 km, about 5.3% of the total length of the Black Sea coast, and is divided into two units, Northern (between Musura Bay and Cape Midia) and Southern (from Cape Midia up to the Romanian-Bulgarian border) units, the latter including the most diverse geomorphology (Panin and Jipa, 1998). To ensure compliance with EU and national laws and regulations, a series of Sites of Community Importance (SCI) were designated since 2007 in the waters of the western part of the Black Sea, some of which were recently designated as Special Areas of Conservation (SAC). In 2016, these sites were expanded, now encompassing an area of 3,580 km^2, accounting for more than 68% of the entire Romanian territorial waters.

Our study focused on two significant Marine Protected Areas (MPAs) from the southern part of the Romanian littoral and shelf area: Underwater Sulphurous Springs from Mangalia (ROSAC0094) and Cape Aurora (ROSCI0281), covering together 193.22 km^2. Both areas have garnered considerable interest due to the documented occurrence of underwater sulphurous springs and of gas emissions, as reported by the scientific community and by scuba divers, while the Underwater Sulphurous Springs from Mangalia (ROSAC0094) was designated to specifically protect the habitats associated with these springs. In addition to the designated MPAs, a series of underwater sulphurous springs occur outside the protected area, extending into adjacent regions.

Our research employed a distinct combination of geophysical (Multibeam Echosounder System) and geochemical techniques (CH_4 measurements), as well as sediment sampling, to map benthic habitats and understand the distribution, composition, and dynamics of these ecosystems.

Underwater sulphurous springs (or seeps) are renowned as biodiversity hotspots in diverse marine environments (Ionescu et al., 2012). According to Zektser et al. (2006), groundwater dynamics in artesian structures adjacent to seas shows that the groundwater flow in the upper hydrodynamic zone is usually directed toward the sea and generates submarine groundwater discharge. Thus, submarine groundwater discharge occurs as concentrated water springs along tectonic disturbances and in karst or fissured zones, or as a result of distributed seepage through low-permeable roofs of aquifers into marine, bottom sediments.

Considering the rock types (sandstone, limestone) and their properties (fractured, karstified), hydrostatic pressure and flow dynamics influence the spring discharge at the surface (Manga, 2001; Pitts and Alfaro, 2001). The position of a spring and its water composition can be constant over time due to stable aquifer hydrogeochemical conditions (Prescott and Habermehl, 2008).

The combined effects of water chemistry and microbial activity lead to dissolution of soluble rocks, forming complex cave systems and other geological features. Notable examples of such systems include Movile and Limanu caves, extensively studied and documented (Horoi, 1994; Sârbu et al., 1996; Sârbu and Lascu, 1997; Onac and Drăguşin, 2017; Sârbu et al., 2019; Drăguşin et al., 2021).

Methane is the third most important greenhouse gas after water vapor and carbon dioxide, and accounts for 20% of the radiative forcing on Earth's climate, while also playing a significant role on tropospheric-atmospheric chemistry (Houghton et al., 2001; Etminan et al., 2016). Oceans and seas are generally considered minor contributors to the total global CH_4 budget, with coastal regions as stronger sources of CH_4 to the atmosphere than open ocean waters. Of the total marine methane release, up to 75% is dominated by shallow coastal environments (Weber et al., 2019), followed by porewater-seawater diffusion, fluid flow, or by ebullition of gas bubbles (Lohrberg et al., 2020). At shallow depths, the efficiency of the water column to reduce CH_4 fluxes is diminished due to limited retention time of bubbles in the water column and to short diapycnal barriers (Lohrberg et al., 2020), leading to CH_4 concentrations in surface waters at 5–20 nmol/L levels (Mau et al., 2007; Borges et al., 2016).

An important pathway for degassing sediments at the seabed-water interface are episodic mud volcano eruptions (Kopf, 2002; Dimitrov, 2002a), either continuous seepage over wide areas or localized gas vents (Etiope and Klusman, 2002). A large number of studies dealing with underwater seeps in various parts of the world (Judd et al., 1997; Hornafius et al., 1999; Clark et al., 2000; Klusman et al., 2000) confirmed elevated methane concentrations in surface waters above such seeps (Cynar and Yayanos, 1992; Ward, 1992). At Mangalia, underwater sulfurous springs drain the regional aquifer that was also studied onshore. According to Sârbu and Lascu (1997), the analyzed water from Movile Cave (near Mangalia) showed concentrations of 200 nM/L CH_4, 300 nM/L NH_4, and 300 nM/L H_2S.

In Mangalia area, sulphurous springs occur in both terrestrial and underwater environments, contributing to its unique bio- and geodiversity. Underwater, the springs with sulphurous properties are creating a diverse hydrochemical phenomenon spanning from the shore line to waters reaching few tens of meters in depth (Figure 1).

According to Brad et al. (2021), the sulphurous springs from Mangalia discharge mesothermal sulphurous water from an aquifer that extends into the continental area over several tens of square kilometers. This water contains high concentrations of H_2S, CH_4, and NH_4, creating a specific chemical composition. The presence of these compounds supports the development of a chemoautotrophic ecosystem, where microbial organisms play a crucial role as primary producers. These microorganisms form floating biofilms on water surface or attached to solid surfaces (e.g., rocks, algae) and serve as a food source for various aquatic and terrestrial invertebrates.

To date, 21 aquatic invertebrate species have been documented and recorded in association with these sulphurous springs (Sârbu et al., 1996; Brad et al., 2021). These species adapted to the specific conditions influenced by the sulphurous springs. The presence of sulphurous water and the microbial activity contribute to extensive hypogene karst features in the area (Onac and Drăguşin, 2017).

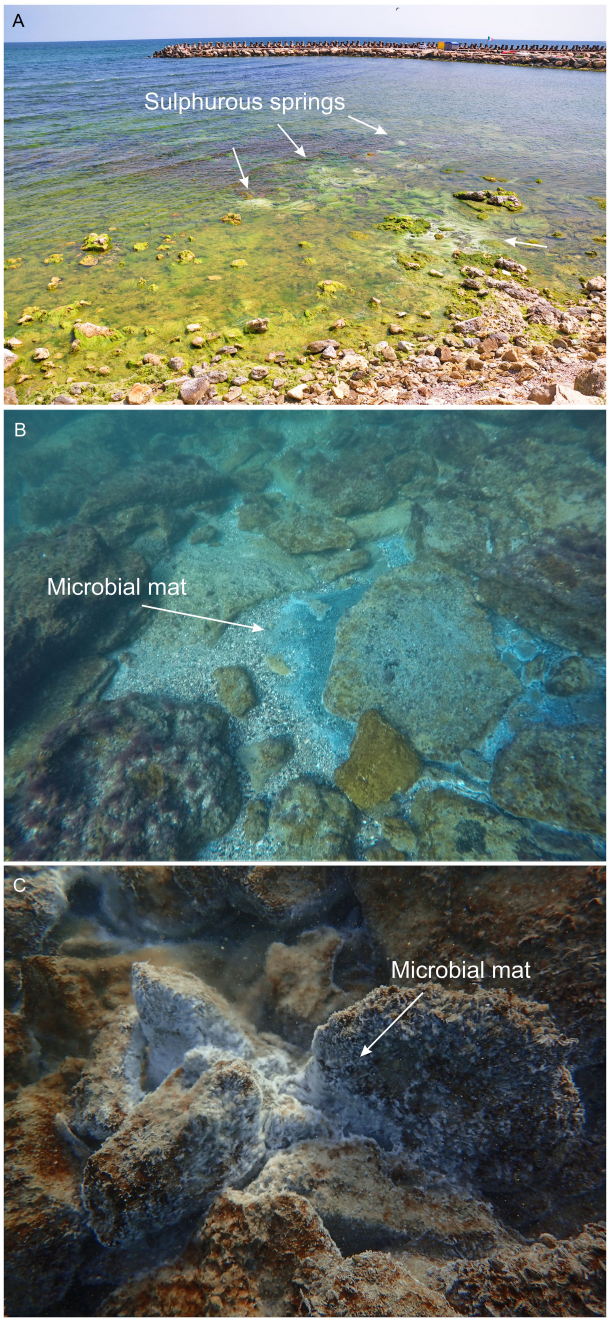

FIGURE 1
Underwater sulphurous springs in the Mangalia coastal area. **(A)** aggregations of near shore springs (Photo: Adrian Popa); **(B)** sulphurous spring in the ROSCI0281 Cape Aurora, Natura 2000 MPA. The image captures the presence of a distinct white microbial biofilm surrounding the spring (Photo: Sorin Balan); **(C)** sulphurous spring in our study area located in the ROSAC0094 Sulphurous Underwater Springs from Mangalia, Natura 2000 MPA. The image showcases a microbial biofilm attached to limestone near the springs (Photo: Mihai Baciu).

1.1 Previous research

In the southern littoral and shelf area of Romania, several investigations have been conducted, although only a few of them had the specific objectives of habitat mapping (Zaharia et al., 2012, 2013; Ungureanu et al., 2015; Begun et al., 2022) or the study of the underwater springs. Some studies were part of national projects led by GeoEcoMar (e.g., PN-1816-0301, PN-1920-0301, PN-1920-0302). The Romanian National Institute for Marine Research and Development "Grigore Antipa" also investigated the small bays along the embankments near beaches or in small areas close to the shore, focusing on habitat mapping and including biology, water chemistry, sedimentology, and bathymetry research for the development of management plans dealing with Sites of Community Importance (SCIs) (Management plan of ROSCI0094).

However, it is worth noting that the only surveys focused on the study of underwater sulfurous springs in the Mangalia area, to the best of our knowledge, were conducted in 2019-2020 in very shallow waters near the shore (Kinkaid, 2020). This implies a limited understanding of the unique characteristics of the underwater sulfurous springs in the region prior to these surveys. None of the previous studies in the southern littoral and shelf area of Romania combined geophysical and geochemical methods, as employed in this study. The combination of geophysical and geochemical methods was chosen in this study for their complementary benefits.

By employing the multibeam echo sounding technology covering large areas, the seeps were identified based on the distinct spikes they generate in the bathymetry data and from the water column data, as this method is highly effective in identifying underwater features and anomalies. Geochemical measurements with a gas analyzer were employed simultaneously to detect spikes in CO_2 and CH_4 gasses, typically associated with underwater sulphurous springs. Measuring the concentrations of these gasses permitted further detection of the seepage activity. Thus, combining the two methods, our understanding on the underwater sulphurous springs was enhanced by recording both geophysical and geochemical data, providing a better assessment of seepages.

Research conducted along the Bulgarian Black Sea coast by the Institute of Oceanology - Bulgarian Academy of Sciences (IO-BAS) highlighted the significance of methane seepage areas as potential earthquake precursors and their contribution to atmospheric methane levels. Their studies identify active seepage and estimate the number of seeps in shallow coastal waters through remote sensing techniques, emphasizing the relationship between gas seepages and earthquakes in marine conditions. Additionally, the estimation of atmospheric methane contribution from gas seepages provided insights into the impact of these seepages on the overall methane budget, for better monitoring tools, for forecasting earthquakes, and for understanding the role of gas seepages in the marine environment (Dimitrov, 2002b; Parlichev and Vasilev, 2021; Vasilev et al., 2021).

Fault systems can provide critical pathways and structures that facilitate the fluids migration and escape, such as natural gas, oil, and other substances reaching the seafloor. These pathways allow the fluids to escape into the water column, forming seep features such as gas plumes, oil slicks, or sediment mounds.

1.2 The sulphurous underwater springs and their relation with benthic habitats in the area

The marine benthic habitats associated with the NATURA 2000 sites ROSAC0094 (Sulphurous springs from Mangalia) and ROSCI0281 (Cape Aurora) in Romania are characterized by the occurrence of mesothermal sulfur seeps across mediolittoral to infralittoral bionomic zones. The seeps can be recognized by the distinct white-grey circular shapes formed by bacterial mats. These springs may have a temporary or permanent functioning depending on the geothermal processes. The waters surrounding the seeps have relatively constant temperatures throughout the year and they typically range from 21-27°C, while the pH is slightly basic, around 7.5 (Kinkaid, 2020). These environmental conditions make the habitats around these springs particular, allowing a limited range of organisms to thrive.

In the proximity of the springs, environmental conditions are suitable primarily for microbial mats consisting of aerobic, sulphur-oxidizing bacteria and other microbes (Sârbu et al., 2019). These microbial mats provide a suitable habitat for a variety of meiobenthic invertebrates, including nematodes and oligochaetes, which have the ability to withstand direct flow of spring water. In some cases, these invertebrates form well-established, highly abundant communities. Seven main benthic habitats are described in the area, following a depth gradient from shore (Begun et al., 2018, 2022).

The emanations from sulphurous springs have a notable impact on the nearby pelagic communities. Large numbers of these seeps in a confined area can particularly influence the abundance and diversity of phytoplankton by providing a rich supply of nutrients (Schubert et al., 2017), fostering the growth of benthic-pelagic communities. Apart from creating a favorable environment for these organisms, the emanations from sulphurous springs can also contribute to the formation of novel geological features, which in turn offer new habitats for benthic species. Consequently, these habitats support a distinctive and diverse ecosystem, and play a significant role in shaping the marine environment in the Mangalia area.

2 Geological framework

The geological setting plays a crucial role in shaping the type and distribution of underwater sulphurous springs. These springs are often associated with fault zones, fractures, or karst systems. The regional tectonic framework, including the arrangement and movement of tectonic blocks, can influence the distribution and activity of the sulphurous springs.

2.1 Geological setting

The study area covers part of the southern Romanian Black Sea continental shelf, in front of Mangalia city and Venus, Cap Aurora and Neptun resorts. Mangalia area is located within the Southern Dobrogea block of the Moesian Platform, a major tectonic unit of the Carpathian-Balkan foreland. The Moesian Platform is characterized by a heterogenous folded basement (Săndulescu, 1984; Seghedi et al., 2005a, b; Oczlon et al., 2007) and a sedimentary cover composed of Paleozoic, Mesozoic, and Cenozoic deposits, separated by unconformities (Paraschiv, 1975, 1979, 1983; Săndulescu, 1984). The Southern Dobrogea block, delineated by the Capidava-Ovidiu Fault to the north, the Intramoesian Fault to the south, prolongates into the Black Sea down to the continental slope, being gradually replaced by an oceanic-type crust (Săndulescu, 1984; Finetti et al., 1988; Visarion et al., 1988; Ionesi, 1994; Dinu et al., 2005).

Geological investigations carried out in the study area, specifically borehole studies (Paraschiv, 1979; Visarion et al., 1979; Krautner et al., 1988; Seghedi et al., 2005a, b; Ion et al., 2003), pointed out an Archaean and Proterozoic basement lying beyond 600 m depth and unconformably covered by Palaeozoic, Mesozoic and Cenozoic sedimentary formations, separated by sedimentary gaps.

The Palaeozoic (Cambrian-Ordovician-Carboniferous) deposits start with marine terrigenous successions (Cambrian-Lower Ordovician), followed by Ordovician-Silurian graptolite shales, terrigenous sequences (Upper Silurian-Lower Devonian), carbonate rocks and evaporites (Upper Devonian-Lower Carboniferous), ending with terrigenous sequences with coal beds (Middle – Late Carboniferous). The Upper Palaeozoic (Permian) – Lower Mesozoic (Triassic) sedimentary cycle includes three main sequences, the lower and the upper being predominantly continental (terrigenous) with an interlayered marine, carbonate-evaporitic succession. Magmatic activity was quite common during the Permo-Triassic interval, especially at the beginning of the Permian and at the Middle-Late Triassic boundary.

The Mesozoic (Jurassic-Cretaceous) formations are mainly marine, dominated by a thick carbonate platform facies (both neritic and pelagic, and reef buildups in Urgonian facies). The Eocene deposits of this sedimentary cycle are predominantly grey and grey-green marls.

The Cenozoic (Badenian-Pleistocene) sedimentary deposits are represented by marls, clays, limestones (locally highly fissured and karstified) and sandstones, overlain by neritic sands, conglomerates and silty-clays. The entire region is underlain by Sarmatian (Miocene) lumachellic limestones with coquina, interbedded with marls (Tătărâm et al., 1977; Ion et al., 2003; Panin, 2005; Briceag et al., 2018). The surface geology of our study area consists largely of Pleistocene loess and loess-like (loam) deposits, a mixture of silt, sand, and clay. The Sarmatian limestones outcrop rarely, while Holocene deposits outcrop along river beds or in the vicinity of lakes (e.g., Mangalia Lake, Techirgiol Lake) (Figure 2).

2.2 Tectonic framework

Tectonics is a major controlling factor of the genesis of the Black Sea Basin, influencing coastlines and sea-level changes through isostatic adjustments. As block tectonics (i.e., horsts and grabens of different ranks delineated by faults and fractures) is a

10.3389/fmars.2024.1414673

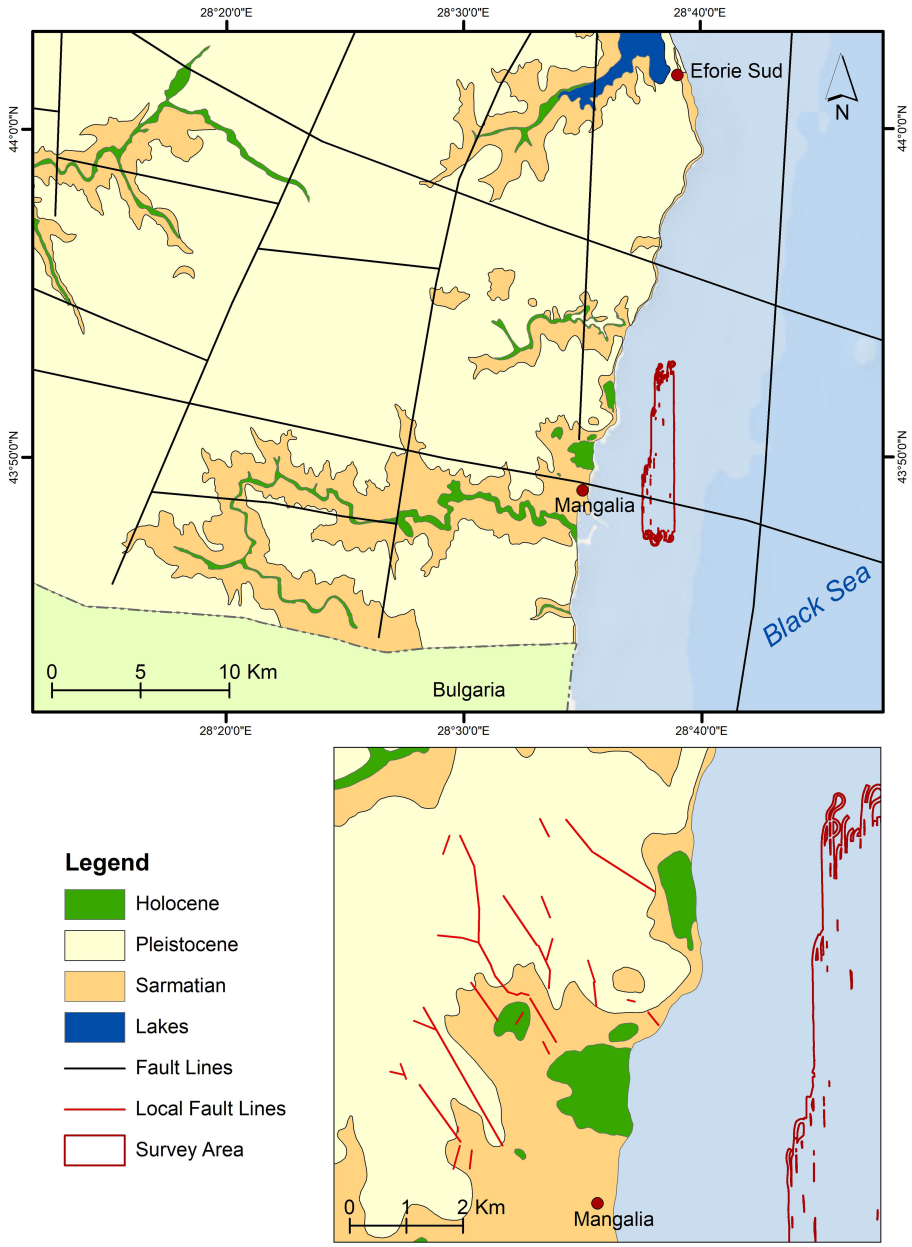

FIGURE 2
Upper image: representation of the known regional fault system (black lines) surrounding Mangalia (compiled after Visarion et al., 1988, 1990; Dinu et al., 2005; Oaie et al., 2016). Lower image: detail on the local faults (red lines) interpreted by Drăguşin et al. in 2021. Background map: ESRI World Ocean Base.

typical feature of the Moesian platform (Săndulescu, 1984; Visarion et al., 1988), it is important to acknowledge several regional fault systems (e.g., black lines in Figure 2) interpreted based on geological and geophysical data by various authors (Săndulescu, 1984; Visarion et al., 1988, 1990; Tari et al., 1997; Săndulescu and Visarion, 2000; Dinu et al., 2005; Georgiev, 2012; Munteanu, 2012; Oaie et al., 2016; Diaconescu, 2017; Diaconescu et al., 2019; Stanciu, 2020; Stanciu and Ioane, 2021a, b): i) a NW-SE (mainly) strike-slip fault system, of ages ranging from Palaeozoic to Cretaceous, transverse to the East Carpathians Bend zone and extending into the Western Black Sea shelf; ii) a NE-SW (normal and strike-slip) younger fault system, some of them generated or reactivated during the Neogene; iii) a W-E fault system; iv) a N-S fault system, along or parallel to the Western Black Sea coast.

Faults provide critical pathways for escape and migration of fluids such as the mesothermal sulphurous waters in Mangalia area, forming springs and seeps.

2.3 Hydrogeological considerations

The Southern Dobrogea Block of the Moesian Platform contains the most important underground water resources of Romania, confined to a regional, transboundary (Romania-

Bulgaria) karstic aquifer system (Dragomirescu, 1927; Capotă, 1980; Zamfirescu et al., 1994; Pitu and Verioti, 2011, 2010; Pitu et al., 2022). The Sarmatian limestones extend in most of the Southern Dobrogea Block and especially in its eastern half. To the south they reach up to 150 m in thickness (Pitu et al., 2022), hosting an unconfined aquifer fed mainly by meteoric waters (Capotă, 1980; Zamfirescu et al., 2010). In the study area, the water belongs to a chloride-sodium type (average mineralization of 1100-1300 mg/l, locally ≥ 4000 mg/l) (Zamfirescu et al., 2010; Pitu et al., 2022).

The Upper Jurassic – Lower Cretaceous carbonate (limestone and dolomite) complex of the Moesian Platform contains a regional-scale deep aquifer, most of it confined, the main aquifer in the study area. It was strongly affected by the NW-SE and NE-SW faults systems, breaking the Upper Jurassic – Lower Cretaceous carbonates in isometric tectonic blocks (Zamfirescu et al., 1994, 2010; Popa et al., 2019) of different sizes, 200-1200 m thick, favoring deep karstic processes (cracks and voids) and water escape along faults (Dragomirescu, 1927; Pitu et al., 2022). The aquifer's main water recharge zone is located south of the study area, in Bulgaria, while the underground water flow is S-N trending, mainly towards the Black Sea coast (Siutghiol Lake and Mangalia area), and secondarily towards the Danube River (Capotă, 1980). The water is bicarbonate, belonging to a calcium-magnesium type (average 450-600 mg/l mineralization and general hardness of 8-26°dH), mesothermal, 20-26°C (Zamfirescu et al., 2010; Pitu et al., 2022).

The W-E hydrogeological cross-section in Figure 3 illustrates the two main aquifers of the Southern Dobrogea Block: the upper, free-flow Sarmatian aquifer discharging into the Black Sea, while the lower, confined, Upper Jurassic – Lower Cretaceous aquifer locally discharge into the Sarmatian aquifer (consequently into the Black Sea) through fault systems, as is the case of Mangalia area.

Due to local geological and/or tectonic conditions, yet to be identified, with very few dedicated geological and geophysical studies and with no clear research related to their origin.

The ubiquitous presence of pyrite (disseminated, in large quantities) in the Sarmatian limestones, gives the sulfurous character of the seeps in Mangalia area, onshore and offshore (Ciocârdel and Protopopescu-Pache, 1955). The same authors mention that due to the exothermic oxidation of pyrite, the ground waters from this area are mesothermal. The mesothermic character of the seeps and springs can be also explained (as an additional process) by the ascending vapors of water, via the regional fractures that are present in the Mangalia area (Slăvoacă et al., 1978).

Graben structures observed onshore at Russalka and Bolata (northern Bulgarian Black Sea coastline, just south of Mangalia area) may suggest a recent extensional regime in this area (Stanciu and Ioane, 2021a). An older extensional regime was possibly associated with magmatic intrusions in Mangalia (Romania) – Shabla (Bulgaria) area, when interpreting high magnetic anomalies onshore and offshore (Stanciu and Ioane, 2021b). This could also explain the high thermal waters observed in boreholes (Benderev et al., 2016) along the northern Bulgarian Black Sea coastline, within Durankulak – Shabla area, as well as the sulphurous mesothermal seeps occurrences in Mangalia area.

The mesothermal (24°-26°C) underground waters reaching the surface onshore and offshore Black Sea in Mangalia area are generating springs and seeps of low mineralization (0,990-1,34 mg/l), hydrogen sulphide (H_2S) in moderate concentration (5,4-17,7 mg/l), low chlorine, sodium, magnesium, iodine, bromine, ammonium and methane (Romanian Ministry of Health, Institute of Balneology and Physiotherapy, 1973; Capotă, 1980; Teleki et al., 1984).

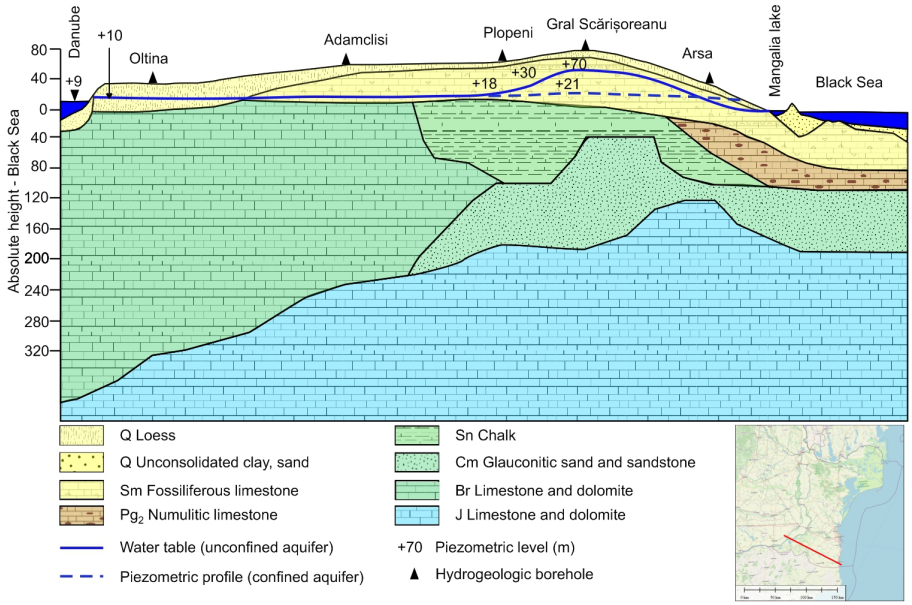

FIGURE 3
Synthetic W-E hydrogeological cross-section of the Southern Dobrogea block (modified from Zamfirescu et al., 2010). Right lower image: Map of Romania (OpenStreetMap) and the location of the cross-section (marked with the red line).

North of Mangalia city, mesothermal sulphurous springs feed small lakes hosted within karst depressions called "obane", supporting abundant vegetation and marshes. The largest doline in this region is Hergheliei Marsh, elliptical in shape (1.62 km long, 1.33 km wide), its eastern part being covered by the Black Sea. Originally, Hergheliei Marsh was circular, its eastern edge being now submerged, 5 m deep and about 700 m offshore (Drăguşin et al., 2023). Its average depth is 1.7 m and it hosts a 7-8 m thick peat deposit (Breier, 1976; Popovici and Jianu, 2006). A ca. 100 m wide sandy littoral belt separates the marsh from the Black Sea, but the original sandy barrier was only about 50 m wide, widened in 1968 for the road and for the infrastructure between Saturn and Venus resorts. The marsh is fed by ca. 25 mesothermal sulphurous springs (Breier, 1976; Popovici and Jianu, 2006) and was originally fully covered by a compact floating reed bed. After dredging works during the late 1980's, only an area of 16 Ha was left in its original state.

2.4 Geomorphological observations

Soft cliffs represented by loess overlying Sarmatian limestones influence the coastal geology and dynamics. The loess cliffs do not exceed 25 m in height, alternating along the shore with small sized, pocket beaches and barriers closing small lakes. As the permeable Cenozoic deposits allow the meteoric water to infiltrate into the Sarmatian limestones, intensive karstic features occur, such as Limanu Cave, dolines, encased valleys such as Obanul Mare, Balta Blebea or the valley hosting Hergheliei Marsh.

Considering the tectonic influence in the local geomorphology, Drăguşin et al. (2021) extracted lineaments of the dolines' long axes and valleys, inferring local fractures. Following the methods used by Williams (1972), Deike (1989) or Öztürk et al. (2018); Drăguşin et al. (2021) emphasized three main trends of such fractures (red lines in Figure 2): a NW-SE and NNW-SSE trend, interpreted as related to the main regional strike-slip fault system and a N-S trend corresponding to the fault system along the Western Black Sea shore. In this study the dataset of Drăguşin et al. (2021) is used and completed with lineaments interpreted in the submerged topography as valleys and outcrop discontinuities, in order to investigate the underwater seeps occurrences with respect to possible tectonic.

Onshore, in the vicinity of Mangalia area, three exokarstic complexes were identified (Constantinescu, 2002): the Movile Complex, containing collapsed dolines, named "oban" in the local language: Obanul Mare, Obanul Mic and Obanul Blebea, and large dissolution dolines, Hergheliei Marsh and Kara-Oban complexes. In the Movile Complex, the major dolines range between 200-600 m in diameter, bordered by an alternation of small dolines (5-30 m in diameter, 3-10 m in depth) and mounds (10-40 m in diameter, 3-8 m in height).

The Hergheliei Marsh Complex is the largest exokarstic complex in the area, with a horizontal extension larger than 1 km. It is fed by few mesothermal sulphurous springs (Lascu et al., 1995) and by sulphurous creeks originating in the Kara Oban Complex, which itself contains several dolines and depressions fed by sulphurous springs.

3 Materials and methods

The research was carried out on board RV *Mare Nigrum*, operated by GeoEcoMar, between 16-22 November 2021 (MN-227 cruise) and between 7-8 May 2023 (MN-240 cruise). During the MN-227 cruise, three areas covering a surface of 57,4 km^2 were surveyed, all of them in marine protected areas. One of these areas covering 13.8 km^2 (area MN-227-A-02) was of particular interest because here we have found indications of underwater springs. The survey of the underwater sulphurous springs covered an area encompassing the coastal areas offshore Mangalia, as well as the nearby Venus, Cap Aurora, and Neptun resorts. This study area partially overlapped with both ROSAC0094 and ROSCI0281 MPAs (Figure 4). A total of 298.8 km of geophysical and geochemical measurement lines were recorded along 35 lines, distanced at 50 m. The measurement line lengths ranged between 3.7 km and 9.8 km, depending on the water depth, with shorter lines closer to the shore and in shallower waters.

The whole area A-02 was first recorded at one time. After first recording the seeps on MBES but also an increased concentration of CH_4 and CO_2 with the gas analyzer, six additional lines were recorded in the area with the highest gas concentration. These lines have between 1.0-1.5 km length, with a 45° shifted direction. Two lines were measured for each N-S and W-E direction and one for NE-SW and NW-SE directions. Separated from these three areas, 86.5 km of lines were surveyed along three profiles parallel with the shore, beginning in the south Romanian waters to the area nearby of Constanţa harbor in the north. Two of these lines pass through area A-02 and one of them is nearby.

During the second cruise (MN-240), the focus was on the area with the highest concentration of seeps. The main objective was the study of the continuity of the seeps while this time we recorded MBES Water Column Data (not performed during the first cruise). During the MN-240 cruise four lines with a length of 1 km of geophysical data, were recorded.

3.1 Multibeam measurements

Geophysical measurements were performed using a Multibeam Echosounder (MBES) Norbit iWBMSh. The MBES has a roll-stabilized head with a variable frequency range of 200 KHz to 700 KHz, emitting 256 or 512 acoustic beams. To achieve higher accuracy and along-track resolution, the swath used was reduced from the maximum of 160° to a range of 135°-140°, resulting less coverage but higher quality data. The sonar head is integrated with a Motion Reference Unit (MRU) while the positioning and heading were assured by a RTK GNSS unit, model Trimble BD982. The

10.3389/fmars.2024.1414673

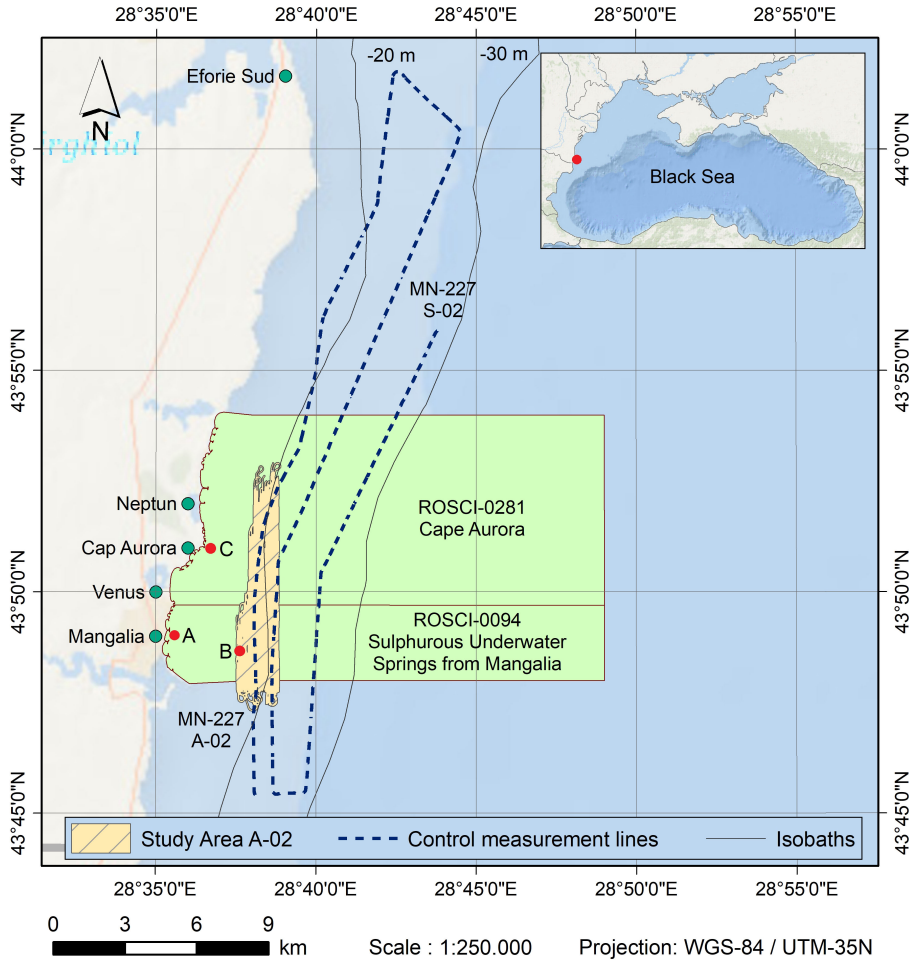

FIGURE 4
The location of the study area within the southern part of the Romanian littoral. The MN-227-A-02 survey area is highlighted in yellow. The dashed lines represent the control measured lines for gases emissions and geophysics data, running parallel to the shore. The Marine Protected Areas (MPAs) are depicted in green, while the most significant cities/resorts in the area are marked with green dots. With red dots are marked photo location for the Figures 1A–C. Background image: OpenStreetMap.

accuracy of roll and pitch measurements, as measured by MV-POSView software, ranged from 0.02° to 0.03°, while the heading accuracy was 0.02°. The GPS horizontal error was reported to be less than 25 cm. The MBES recorded bathymetry, backscatter, and water column data during the survey. Xylem Hypack Hysweep Suite, QPS Fledermaus, and ESRI ArcMap software were used for navigation, data recording, and data processing purposes. Water column was recorded and analyzed using the Norbit WBMS GUI software. During the processing of the multibeam data (bathymetry and backscatter), two software programs were employed: Hypack MBMAX64 and Geocoder. The parallel processing approach allowed for a clearer visualization of the differences in seabed height and sediment type and the identification of spikes in the data (Figure 5).

Spikes in the bathymetry data can have different origins, including differences in acoustic impedance between different mediums such as seawater and gasses or potential system errors. The very high contrast between the acoustic impedance of gases (CH_4, H_2S) and the seawater plays a key role in mapping the seeps originating from the sea floor. In the processing phase, special attention was given to identifying and eliminating spikes caused by system errors. These errors were characterized by their consistency on the same beam and multiple pings and did not exhibit a random distribution like spikes originating from the natural sources. Spikes that were observed on a single ping or beam were disregarded as they were not considered relevant for the study and did not provide a clear indication of an underwater seep. The spikes in bathymetry data were detected from the sea bottom up to few meters from the water surface. Bathymetric map and backscatter mosaic were processed onboard of the research vessel and sediment sampling locations were chosen based on them, collecting samples for each type of detected backscatter of acoustic signal excepting rock outcrops.

3.2 Sediment sampling

The sediment sampling was performed using a Van Veen grab (VVG) at the first 20 cm of the water-sediment interface. The

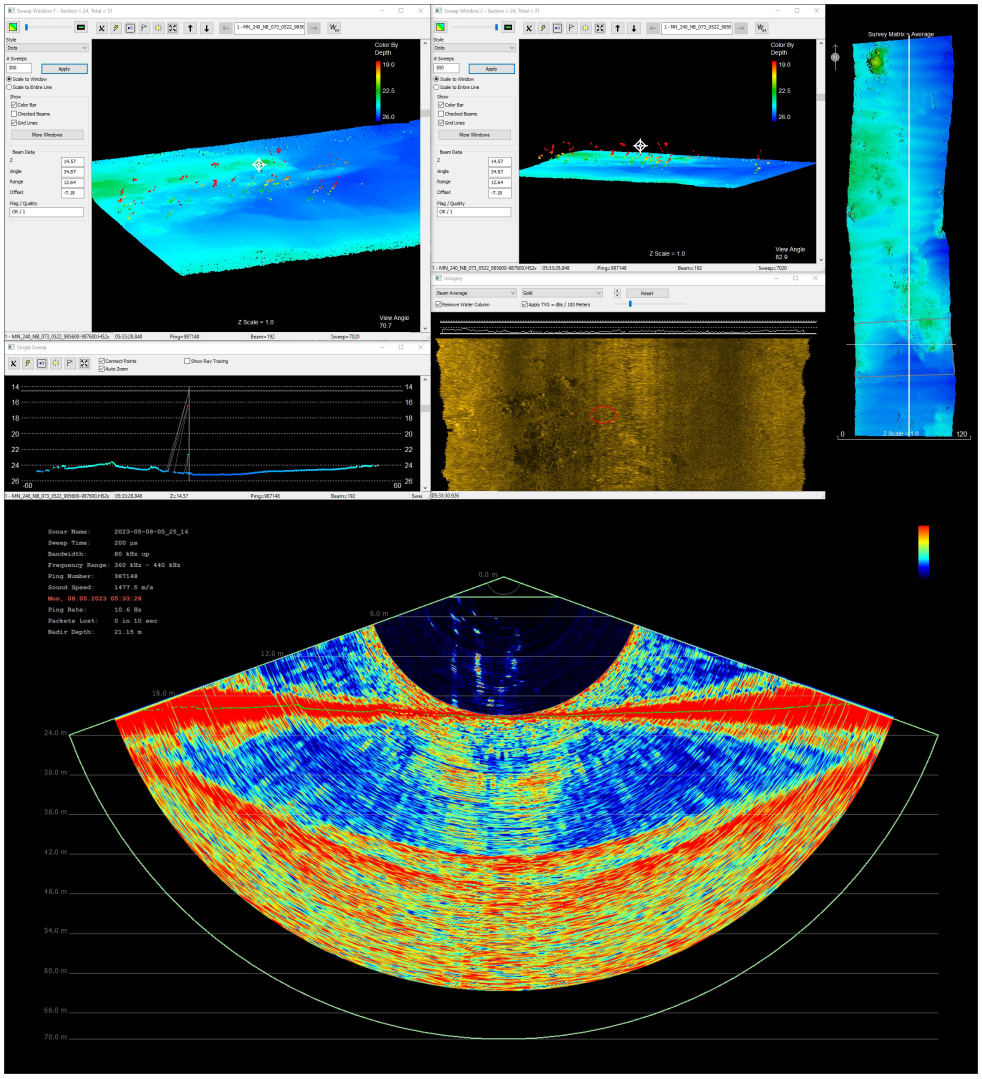

FIGURE 5
Visual representation of underwater seeps/springs using three different types of data: Upper three images - underwater topography and depth of the seabed in the vicinity of the seeps/springs; Left-middle image - transversal profile which displays a cross-sectional profile of the seafloor; Right-middle image - backscattered acoustic energy from the seafloor; Lower image - water column data with emanating seeps. The acoustic ping represented in water column data is marked with a crosshair in the bathymetry data and red circle in backscatter data.

samples were weighted on board of the ship for the shell vs. sediment mass ratio. After the separation of the shell content, particle size analysis of the sediment samples was performed in the laboratory by the laser-diffractometry method using an analyzer Malvern Mastersizer 2000E. The diffractometer can measure the percentages of sediment particles in the various dimensional classes in 0.0001-1.0 mm interval with an accuracy error of 1%. The separation of the granulometric classes conforms to the Udden-Wentworth logarithmic scale (Udden, 1914; Wentworth, 1922): clay, silt, sand, and elements bigger than 2 mm, mainly represented by shells or shell debris. Sediment classification was performed/adapted using the Folk diagram (Folk, 1954) while the textural parameters were calculated using the GRADISTAT package for the analysis of unconsolidated sediments (Blott and Pye, 2001). The results were considered for correlation between the sediment classes with the backscatter mosaic and are presented in a simplified form in Table 1.

3.3 Physical habitat map

Besides the depth of the sea bottom, the MBES records other valuable information such as the backscatter value of the acoustic signal which can be used to produce the physical habitat map. The

10.3389/fmars.2024.1414673

TABLE 1 Study area samples used for correlation of sediments with backscatter.

Sample	Shells (%)	Sand (%)	Silt (%)	Clay (%)	Folk Classification
S18	42.26	6.54	39.54	11.67	shell debris with mud
S19	0.48	43.54	45.89	10.10	sandy mud with rarely shell debris
S20	0.97	73.48	19.91	5.63	muddy sand with rarely shell debris
S21	32.80	54.29	10.03	2.88	shell debris with muddy sand
S22	33.92	55.11	8.50	2.47	shell debris with muddy sand
S23	39.09	48.01	10.21	2.69	shell debris with muddy sand
S24	39.14	20.96	29.92	9.97	shell debris with sandy mud
S25	71.27	16.37	10.18	2.18	shell debris with muddy sand

backscatter strength, calculated in decibels (dB) was used to create a referenced grayscale image (mosaic) with every pixel having an acoustic backscatter strength value. High decibel values indicate coarse particles as tough surfaces (rocks or shell debris) return stronger backscatter reflections of the acoustic signal and are represented on our mosaic as lighter colors, while low decibel values indicate softer sediments (mud, sand) and are represented as darker colors. Different techniques for classifying sediments exist nowadays each with its advantages and disadvantages. For this study, the physical habitats were classified in three broad classes: soft sediments (sand to sandy mud), shell debris and rocky bottom as it was fast and fit well for our purpose.

The physical habitat map was produced through a series of processing stages, first in Geocoder for realizing the backscatter mosaic and after through different functions in Esri ArcMap software for allocating a sediment class to every pixel in the mosaic. The backscatter mosaic was created in Geocoder using bathymetry data processed with MBMAX64 and snippet data recorded with Hypack Suite. Then, the backscatter mosaic, exported as *.geotiff files from Geocoder, were imported in ESRI ArcMap and processed with Focal Statistics function for hard sediments (rock outcrops) while the Map Algebra-Raster Calculator function was employed for the soft sediments (mud, sand, shell debris). The resolution for the backscatter mosaic is 0.4 meters/pixel, while for the sediment cover map a 1.0 meters/pixel was chosen. The last stage implied the transformation of all raster layers to polygon layers and the statistical analysis related to the sediment cover (areas, percentages) for all types of sediments.

3.4 Gas measurements

The continuous CH_4 measurements of surface water was carried out in parallel with the bathymetric profiles with a cavity ring-down spectroscopy (CRDS) gas analyzer coupled to an air-water equilibrator system and a water system feed. The CRDS instrument used for measurements of CO_2, CH_4, H_2O in this study was a Picarro G2301 analyzer (Santa Clara, CA) designed to measure CH_4 in air in the range of 0–20 ppmv, though instrumental specifications (e.g., drift<3 ppbv over 1 month) are only guaranteed in the 1–3 ppmv range. Due to higher concentration of CH_4 in the Black Sea, especially on the coastal area, the instrument was modified at request by the manufacturer with an additional extended range mode for determining CH_4 up to 1000 ppmv.

For air-water equilibration an Amiston Ltd. Air Water Equilibration System (AWES) based on a membrane contractor (3M^{TM} Liqui-Cel^{TM} MM-1.7x5.5 Series Membrane Contactor) was used. The AWES receives water at 2.5 L/min flow and equilibrates this water with ambient air. The equilibrated air is then dried with a Nafion membrane and then flows to the gas analyzer for measurement. The source of counterflow gas required for the Nafion membrane is the exhaust gas from the analyzer pump. A "Drierite" column was used in the counterflow circuit to reduce the water vapor. The air is pulled through the AWES by the analyzer pump. For air samples necessary for equilibration an inlet located at the bow of the ship was used in order to avoid any contamination.

Water is pumped to the laboratory from the intake located on the ship keel at 1.5 m water depth at a flow rate of 30 L/min. In the laboratory, a system to reduce the flow rate necessary for air-water equilibrator was used. For the measurements of water temperature and salinity before entering the AWES system a Hanna HI 9829 multiparameter logging system was used, with a resolution 0.01°C for temperature and 0.001 mS/cm for conductivity. Wind speed, direction and other meteorological parameters measurements were carried out with an Airmar 220WX-IPX6 station mounted on the ship.

The CH_4 concentration values in water obtained using the CRDS analyzer, expressed in ppm, were converted to molar units (i.e., nmol/L) by Henry's law (Equation 1) as the best fit for gas/liquid equilibria and the Henry's constant for molar concentration and partial pressure conversion. It is assumed that the gas content in the membrane equilibrator is equivalent to that in the water phase and CH_4 measured by CRDS analyzer is considered as the real-time concentration of CH_4 in water. The membrane contractor in the equilibrator is maintained at ambient pressure. Also, the water temperature is measured in the same parcel of water just before reaching the equilibrator. For each calculation, Henry's law constant is corrected by the measured temperature at atmospheric pressure.

$$C = p \times K_H \quad (1)$$

In the Equation 1, C is the concentration of CH_4 (mol/L), p is the partial pressure in unit of atm (1 atm = 10^6 ppm) of CH_4, and K_H is the temperature dependent Henry's law constant that is

corrected following the van 't Hoff equation (Sander, 2015):

$$K_H = K_H^{\star} \times exp\left[\frac{-\Delta_{sol}H}{R} \times \left(\frac{1}{T} - \frac{1}{T^{\star}}\right)\right] \quad (2)$$

where K_H^*, in the Equation 2 is the Henry's law constant at the reference temperature, 298 K, T* is the reference temperature, 298 K and T is the measured temperature in water (K). The temperature dependence of the equilibrium constant, $\frac{-\Delta_{sol}H}{R}$ does not change much with temperature and is tabulated (Sander, 2015). K_H also varies with pressure, but because water was taken at a depth of ~1.5m, atmospheric pressure was assumed.

4 Results and discussions

The data from the multibeam echosounder (bathymetry, backscatter, and water column) and from the gas analyzer (CH_4 measurements) was processed and coupled with data from the samples (sedimentology and biology) taken with the Van Veen grab (VVG).

4.1 Lithology of the studied area

The study area was situated on the Black Sea shelf, 1.8-3 km east from shore, closer in the northern part. The water depth varied between 17-29 meters, with the shallowest waters in the western part, closest to the shore, and the deepest waters in the south-eastern part. The sea bottom slope was less than 1° in all areas, excepting rock outcrops. The rock outcrops cover a total area of 2.439 km^2 (17.9%), while shell debris sediments cover an area of 7.266 km^2 (53.3%), mostly close to the rock outcrops with intercalated finer sediments (sand and muddy sand), covering 3.926 km^2 (28.8%). No relation between water depth and the sediment cover was identified. The rock outcrops are highly important for marine life as shelter habitats (Teacă et al., 2006, 2020; Drăguşin et al., 2023), but are also important for sulphurous springs as they emanate through cracks and faults, in the hard sediments.

The distribution of the sediment cover is directly dependent of erosional and depositional processes, also of the relief morphology shaped during the last glaciation, when the shelf surface was exposed (Ross and Degens, 1974; Ryan et al., 1997; Major et al., 2006). Rocky bottom areas occur all over the study area having a random spatial distribution. The sea floor covered by shell debris occurs in almost all cases nearby the rocky bottom areas or at a maximum distance of 400-500 m from them, while finer sediments can be found most of the time at greater distance from the rocky bottom areas.

In the western part of the study area, the apparently random erosion might be the result of the horizontal bedding of the carbonate rocks. In the eastern part, the strata appear to be sloped, with outcropping layer ends, and subject to differential erosion (Figure 6). Presuming that the underwater rock outcrops

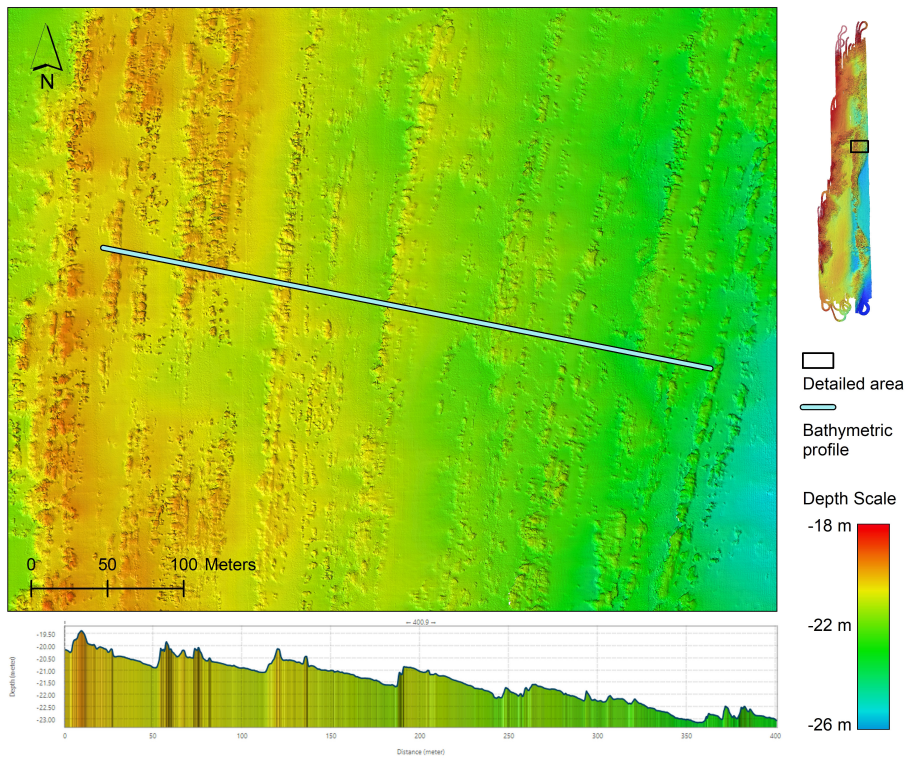

FIGURE 6
Bathymetric profile in the north-eastern part of the MN-227-A-02 survey area represented by the blue line in the upper part of the image where we can see differential erosion related to the mechanical resistance of the different rock types. In the lower part of the image, we can see the rock strata inclination.

are a continuation of the onshore rocks, this may be related to different resistance to erosion for different types of strata, limestones or marls. The difference between the rock strata strike and bedding between the east-side and the west-side of the study area could be caused either by: a) different lithology/facies of the rocks; b) a fault line (Figures 7, 8), partially submerged, apparent on the seabed only in the central and northern parts of the area A-02.

The rock outcrop found in the eastern part forms a block apparently bordered both in the western and eastern parts by faults (Figure 7). For convenience, the fault west of the block was named F1, and the fault east of the block was named F2. While the F1 fault has a north-south general direction, the F2 fault is curved and its direction suggests extension outside the study area.

Another area with inclined, parallel layers occurs in the south-western part of the study area, bordered by soft sediments in the southern part, and by horizontal rock sediments in the northern part. This area is approx. 500 m in length, in a north-south direction, and 100 m wide in a west-east direction, and is a significant source of underwater seeps. We consider this area to be affected by faults in eastern, western, and northern parts or to being affected differently by erosion due to different lithology/facies than the surrounding rock areas (Figure 7).

4.2 Dolines

An exokarstic complex, about 500 m diameter, was identified in the seeps sector 1, at 21-25.5 m water depth, in the eastern part of the study area. This is morphologically partly similar to the complexes identified onshore, in Mangalia Area (i.e., Hergheliei Marsh Complex) (Figure 8). The form of the exokarstic complex is circular, the inner part sediment cover represented mainly by shell debris and less by rocky bottom. At the northern and eastern edges of the complex a series of seeps were detected.

4.3 Pockmarks

Pockmarks are circular or sub-circular seabed depressions, generated by fluids escaping through the sea floor, thus indicating

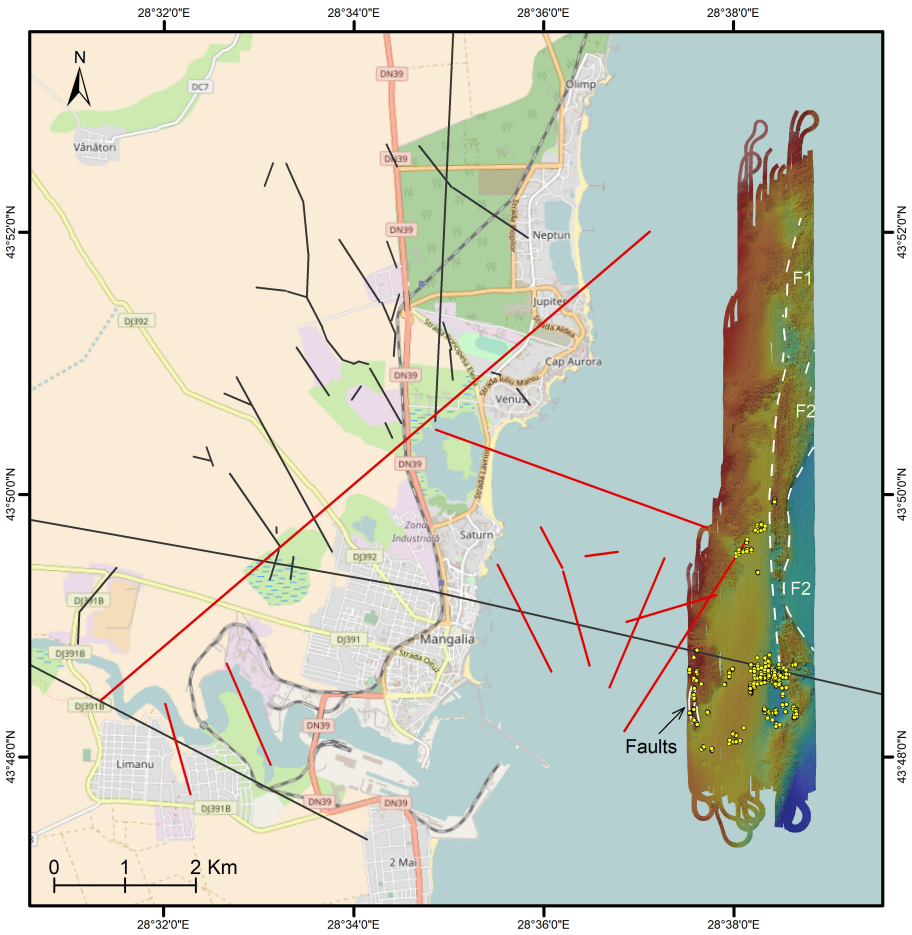

FIGURE 7
Regional fault system in Mangalia area (black lines-compiled from Dinu et al., 2005; Oaie et al., 2016 and Drăguşin et al., 2021) and the new faults depicted by current study (red lines). The green lines show new (presumed) fault lines based on the new bathymetric data acquired in the MN-227 cruise. Yellow dots show the spikes in bathymetry data generated by the emanating fluid seeps. Background map: OpenStreetMap.

10.3389/fmars.2024.1414673

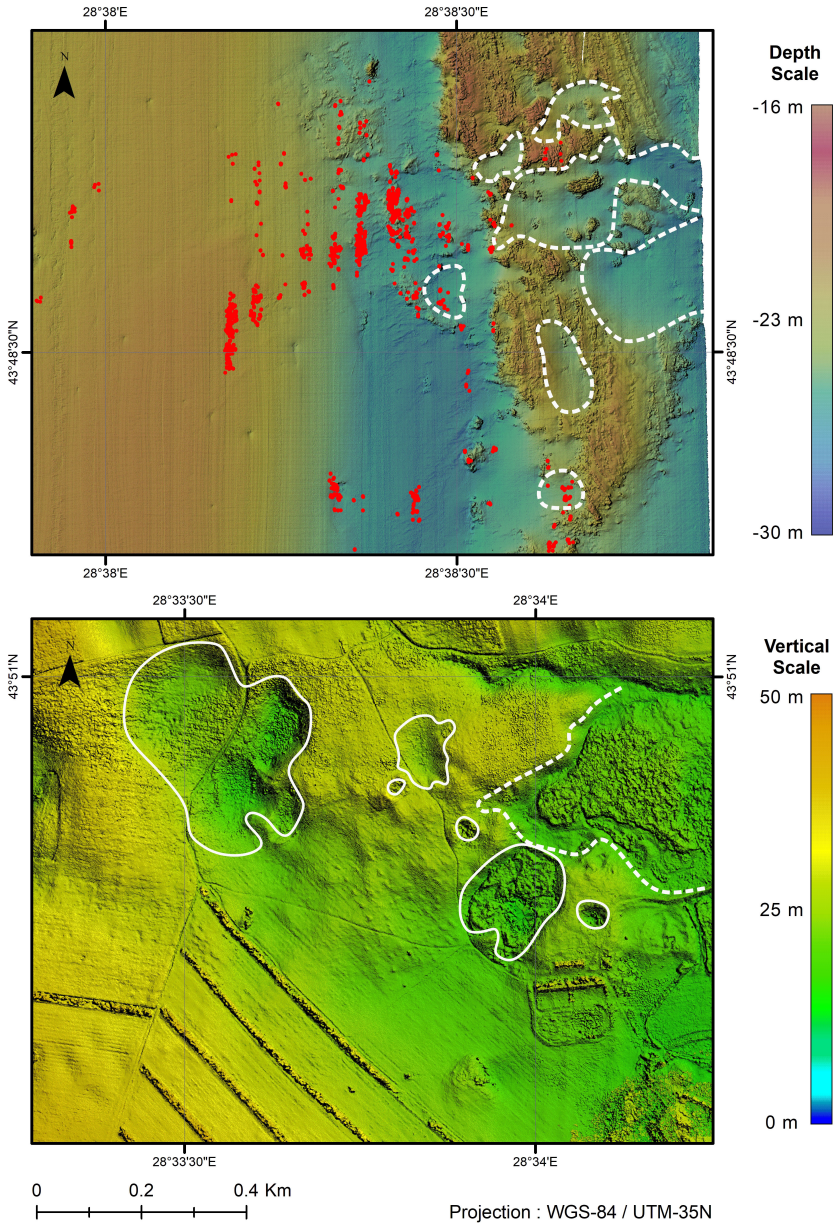

FIGURE 8
Comparative morphology of sea bottom versus the land area nearby Mangalia. Upper image shows the sea bottom morphology in the area where most spikes were detected by geophysical methods and the highest concentration of CH_4 was recorded with the gas analyzer. In the lower image a high-resolution digital surface model of the karst area around the Kara Oban doline, on the NW outskirts of Mangalia is pictured, where sulphurous springs are active (data source: Drăguşin et al., 2021). The hydrology and morphology of the karst depressions seems to have been affected by the construction of levee roads that allowed for water stagnation and reed beds development that hide the true depth of the depressions.

fluid seepages. As fluid flows are a common phenomenon in sedimentary basins (Tasianas et al., 2018), the pockmarks may appear in many areas, ranging in size from a few meters to a few hundred meters (Judd and Hovland, 2007). In the southern part of the study area, pockmarks were detected in areas covered by fine sediments. These areas are identified on bathymetric maps as small seabed depressions, 2-6 m in diameter, rarely up to 10 m, and 10-40 cm level difference. In the overall area, 59 of these features were detected, where the sediment cover is composed of fine sediments (sandy mud). Most of them (53 of 59) were found in the southern part of the study area. These pockmarks are observed both on the bathymetric map having a specific morphology, and on the backscatter data as small spots of brighter color on the mosaic (Figure 9). Some of the pockmarks occur in the same spots where fluid seeps were detected, indicating that they are still active, still most of them do not show evidence of seeping activity at the moment of survey.

4.4 Underwater (sulphurous) springs

Underwater springs were detected in five distinct sectors. Four sectors are identified in the southern part of the study area, offshore

10.3389/fmars.2024.1414673

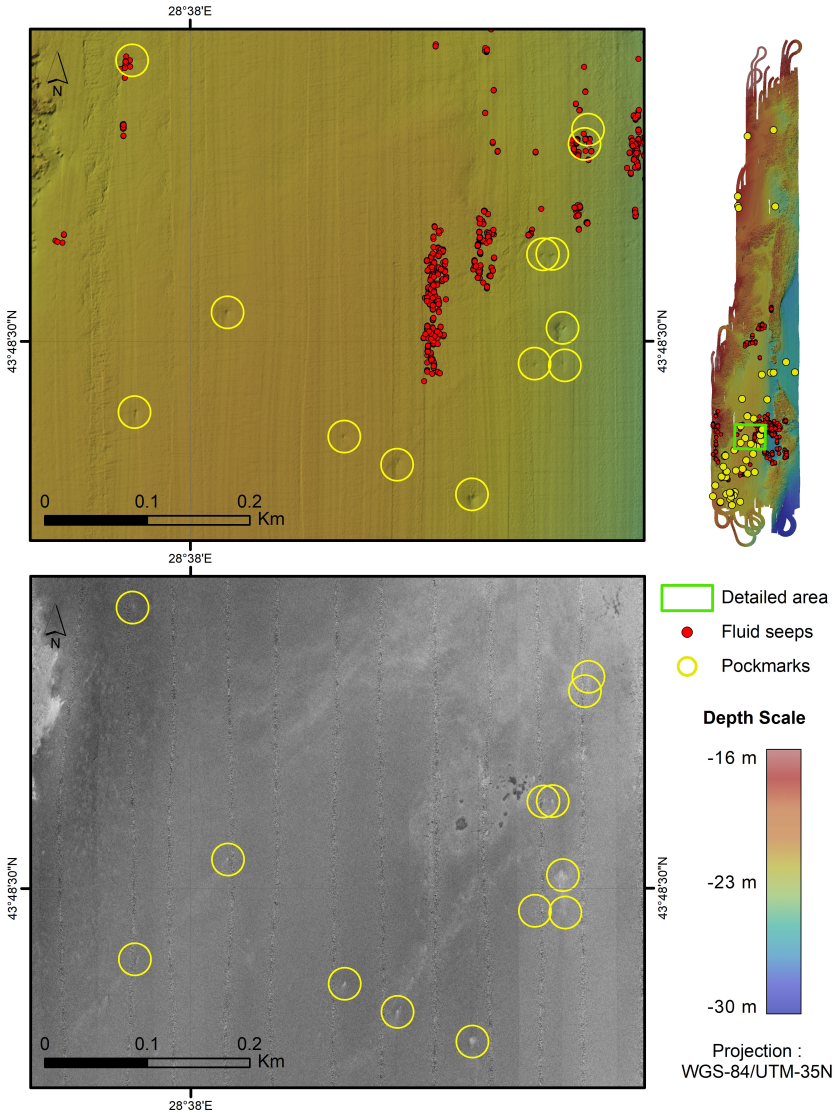

FIGURE 9
Detected pockmarks. Left upper image: Bathymetric map with the pockmarks (showed in a yellow circle) and fluid seeps (represented with red dots). As can be seen some of these pockmarks are correlated with active fluid seeps while most are not. Lower image: the pockmarks appear as brighter spots on the backscatter mosaic. Right upper image: general map of the study area with markers for the fluid seeps and for the detected pockmarks.

Mangalia city, and the fifth sector north of these, offshore Saturn resort. The first sector, containing the most seeps, is located 4 km offshore Mangalia, at 21-24 m water depth (Figure 10). Here, with the MBES system, spikes on all measured lines were recorded, on an area covering about 3 km^2. More than 90% of all spikes were recorded here, therefore this sector is considered to be the most active for fluid seeping (gasses with water or only gasses) in the study area. Most spikes in this sector are located in its northern part, located at the intersection of a fault line crossing in a W-E (103°) general direction (Figure 7), with a presumed fault line along a north-south direction, based on the bathymetry data.

The seeps are located in an area which marks the contact between consolidated rocks and unconsolidated sediments (i.e., sand and shell debris). Most of the seeps are located in the northern part of the sector. The seeps originate mostly from the sea bottom covered with sand or shell debris, except for the western part of the sector where the sediment cover has a higher percent of silt and clay (Figure 11). The rest of the seeps occur concentrically, west, south, and east of the first cluster, suggesting a doline.

The second and third sectors are located to the west (sector 2) and south-west (sector 3) of the first sector, in an area covered by fine sediments (i.e., sandy mud or muddy sand), with a water depth of 20-21 m. The seeps in sector 2, recorded on four bathymetric measurement lines, have a diagonal inline arrangement suggesting a fault line under the sediment cover, although this fault could not be inferred from bathymetry or backscatter data.

The fourth sector is located in the eastern part of the study area, over the bedrock outcrop, with the seeps on north-south trending. The seeps were detected on three measurement lines, at water depths between 15-19 m. This sector was divided into two clusters based on the local lithology and on the quantity and dispersion of fluids. The north cluster (4N) has rather low emissions of fluids,

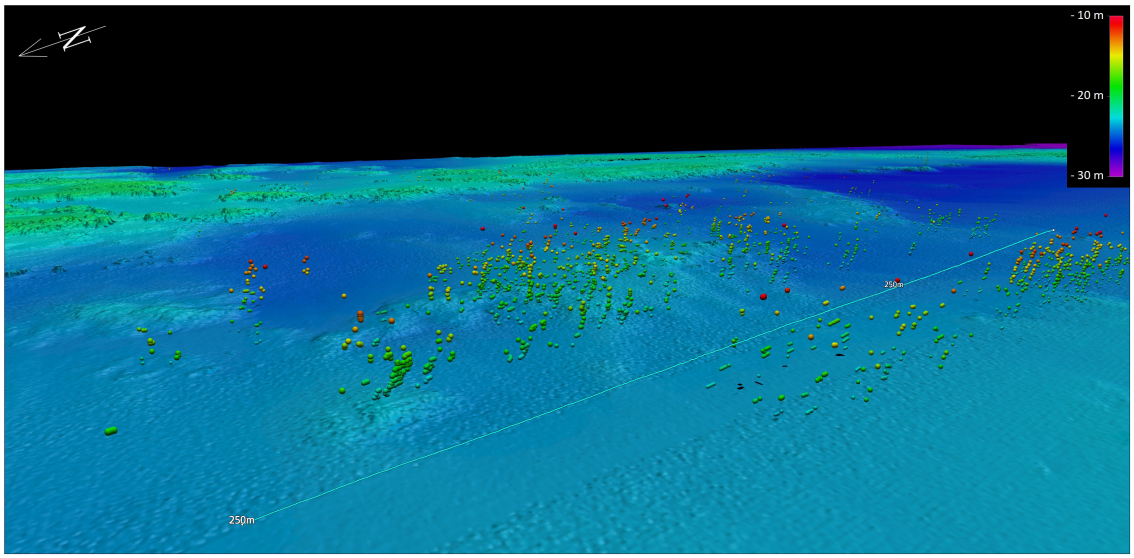

FIGURE 10
MBES detected seeps in Sector 1. Background: bathymetric map build on MBES data recorded in MN-227 cruise.

with seeps dispersed on a few tens of meters, and a random distribution. The rock strata found here appear to have a horizontal orientation, as a result of erosion observed on the bathymetry data (Figure 12). The seeps of the southern cluster (4S) were detected mostly at or near the contact between bedrock and the nearby shell debris sediments. The rock strata appear to have inclined positions, as parallel layers of rock were interpreted based on bathymetry data. The elevation of this bedrock block and the difference of the rock strata positions suggest that it is either affected by faults along its eastern, western, and northern sides (Figures 11, 12) or having a different lithology and facies resulting in different erosion.

The fifth sector (northern sector) is located near the central part of the study area, offshore Saturn resort. The water depth ranges between 21.5-22.5 m, while the sediment cover is represented by fine sediments (sandy mud). The seeps were detected along several measurement lines and they have a general orientation NE-SW while bordering an area covered by rock strata and debris shell sediments. The position of sediments is in line with an interpreted fault line, as inferred by Drăguşin et al. (2023) from previously published bathymetry data (Figure 7), and near the fault line between the western (horizontal) and eastern (subvertical) blocks of rocks (fault F1).

In sector 1 we detected the most spikes (4918 from 5324 spikes in bathymetry data). As seen on the histogram (Chart 1), we detect spikes up to less than 9 meters water depth with a gradual increase in the detections to 17-19.5 meters water depth, then we can see a decrease in detected spikes. Most spikes were detected between 14.5 to 22.5 water depth. In sectors 2 (90 spikes), 3 (90 spikes) and 5 (184 spikes) (Chart 2) most spikes were detected at water depth between 14 to 19,5 m, with only a few detections in water depth of less than 14 m. In sector 4, given the elevated terrain the detected spikes range from 12 to 18 meters water depth, with a few detections between 11-12 m water depth. Except the first sector where we detected many spikes in water depth less than 12 meters (more than 200) in the other sectors few were detected (10 spikes in all sectors).

A density map of the fluid seeps based on the number of spikes recorded was produced with the Blue Marble Geographics Global Mapper software. While it does not show the precise density of the fluid emissions or the quantity of the fluid expelled, this map emphasizes the difference between the areas with a high density of gas seeps and the rest of the study area, contributing to a better understanding of their spatial distribution (Figure 11).

From the total of 5524 detections/spikes, 1980 (35,84%) were detected above soft sediments, 1626 (29,44%) were detected above rock outcrops and 1918 (34,72%) were detected above shell debris. Still, we have to take into consideration that most probably the shell debris and the soft sediments may form only a thin cover (no more than a few to several meters) above the underlaying rocks, the origin of the seeps being the same for all. The presence of the seeps may influence in different ways the different type of sediments.

The final results of the geophysical study were presented in the bathymetry map (Figure 12), backscatter mosaic (Figure 13), physical habitat map (Figure 14). Study area samples collected with the Van Veen grab are presented in Table 1. Gas concentration map for CH_4 (Figure 15) was produced with Blue Marble Geo Global Mapper 22 software and Esri ArcMap software.

4.5 Methane

Seawater CH_4 concentrations at equilibrium varied greatly around a mean value of 10.018 nmol/L within the study area, ranging from 4.168 nmol/L near atmospheric equilibrium to a peak value of 95.608 nmol/L. A difference between the northern and the southern parts of the study area was identified, marked by background values between 7-8 nmol/L in the north and slightly higher values (8-9 nmol/L) in the south.

10.3389/fmars.2024.1414673

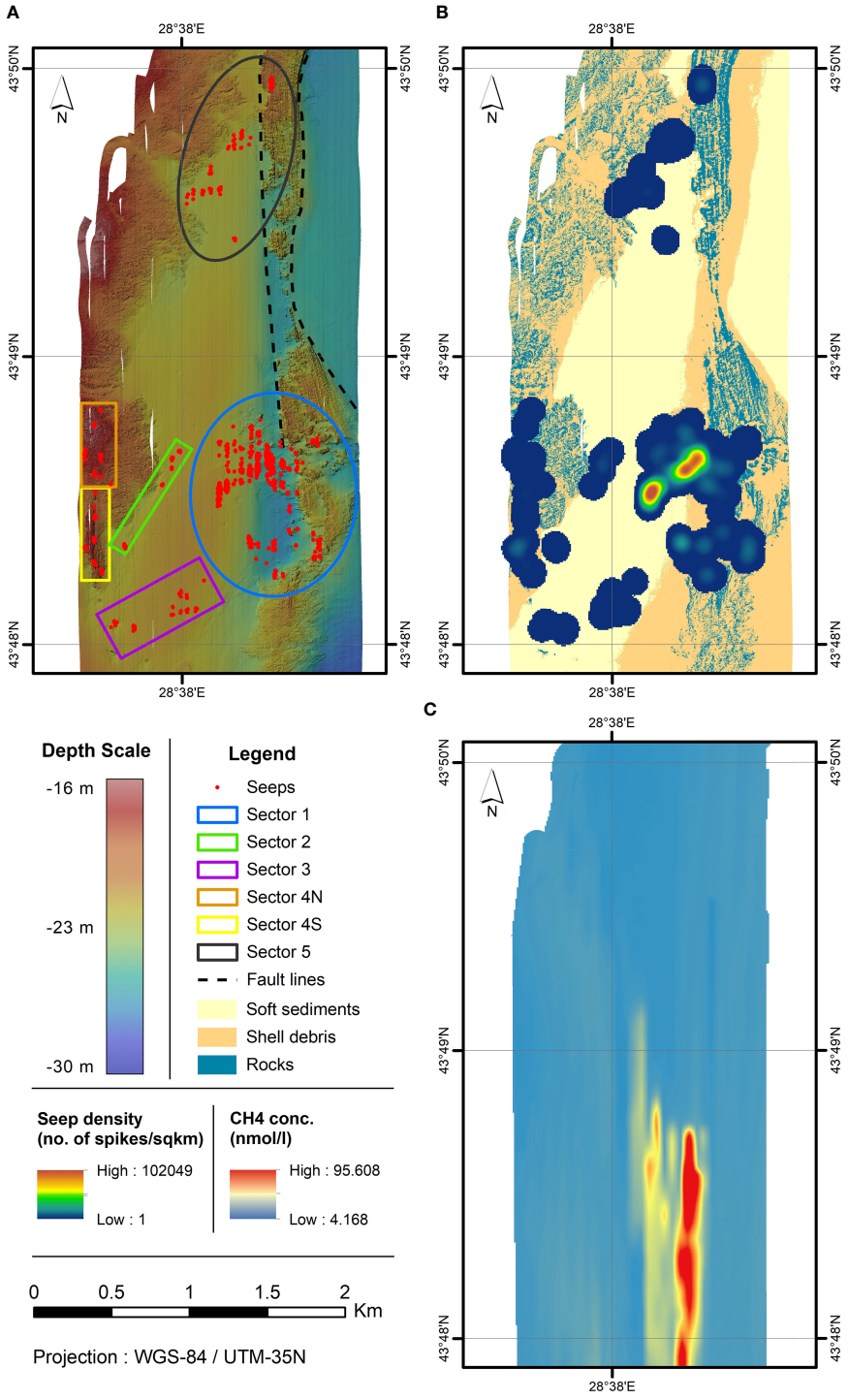

FIGURE 11
Visual representation of seep location within the study area: upper left image **(A)** - bathymetric map of the area with seeps locations, marked sectors and the presumed fault line; upper right image **(B)** - relative density of the seeps (measured as the number in spikes per square kilometer) superimposed on the sediment types coverage of the sea bottom. In the area showing no seep density coverage, we did not detect any seeps. Lower right image **(C)** shows the CH_4 concentration in nmol/l measured with the Picarro G2301 analyzer.

Atmospheric CH_4 mixing ratios showed relatively low variations between 1.867 ppmv and 2.276 ppmv (mean value of 1.993 ppmv) close to the global monthly mean value for November 2021 reported by NOOA (Lan et al., 2023). The salinity of seawater recorded during the MN-227 cruise showed a slight variation between 15.150 PSU and 19.421 PSU indicating an intrusion of water masses from open sea to the coastal area. Also, a slight variation was recorded for seawater surface temperature from 12.99°C to 14.360°C, related to diurnal variations.

10.3389/fmars.2024.1414673

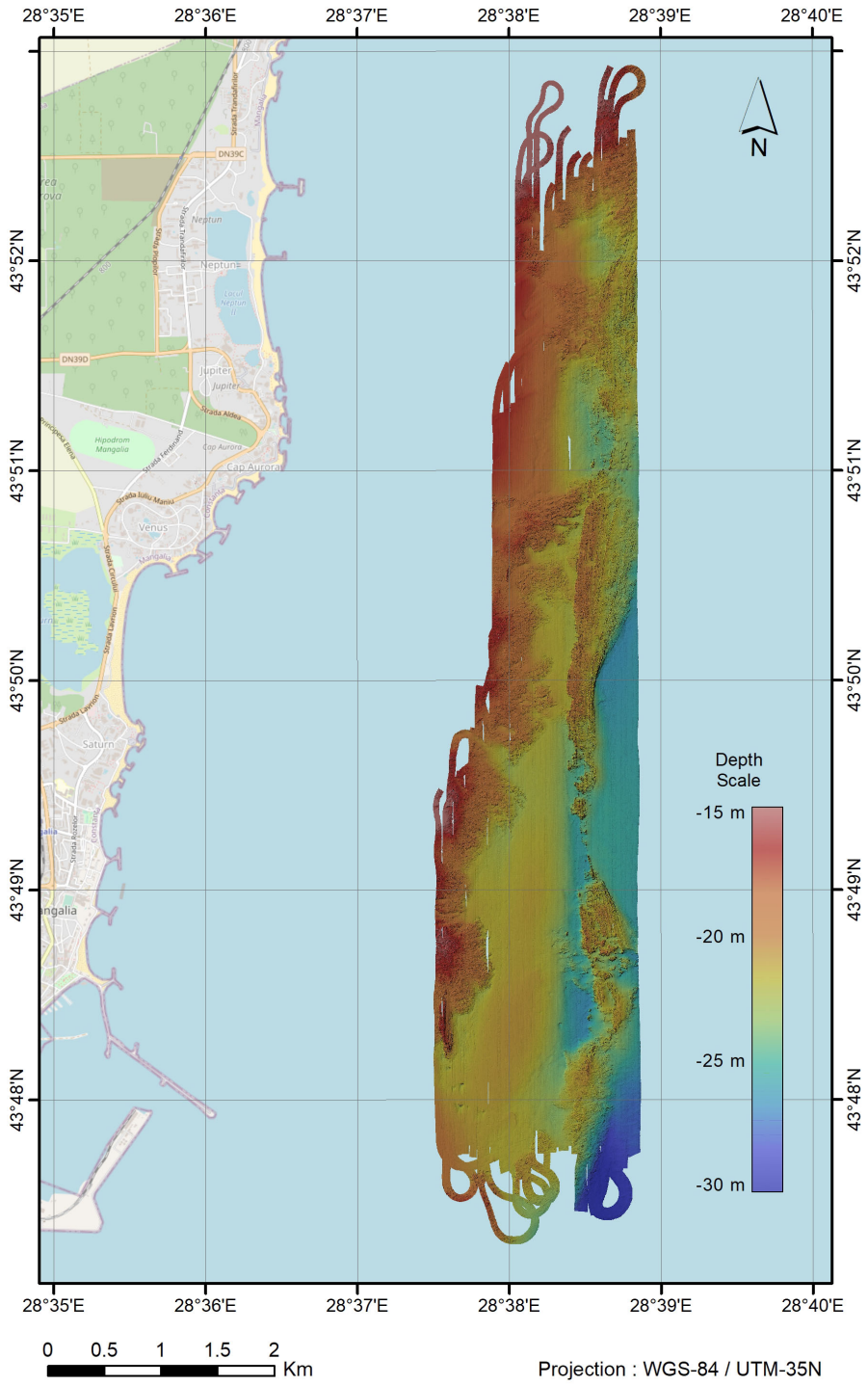

FIGURE 12
Bathymetric map of area MN-227-A-02.

The data across the investigated area reveal a relative uniform distribution of CH_4 concentrations excepting for the south-eastern part, where the highest recorded CH_4 values indicate a hotspot (Figures 11, 15). Here, the highest concentration of CH_4 (95.608 nmol/L) was recorded along a line crossing the cluster with the most spikes in sector 1, supporting the interpretation of geophysical data as the area is affected by gasses in the water column.

A second hotspot occurs 0.5 kilometers south of the first one, along the same line of measurements, defining a second cluster with a lower number of seep emissions. The recorded CH_4 values range between 45-57 nmol/L, with a similar spatial extension. The third hotspot was recorded at about 700 m south from the second one, along an adjacent line to the west, with CH_4 values between 45 and 61 nmol/L, and about 400 m in length. This hotspot was recorded

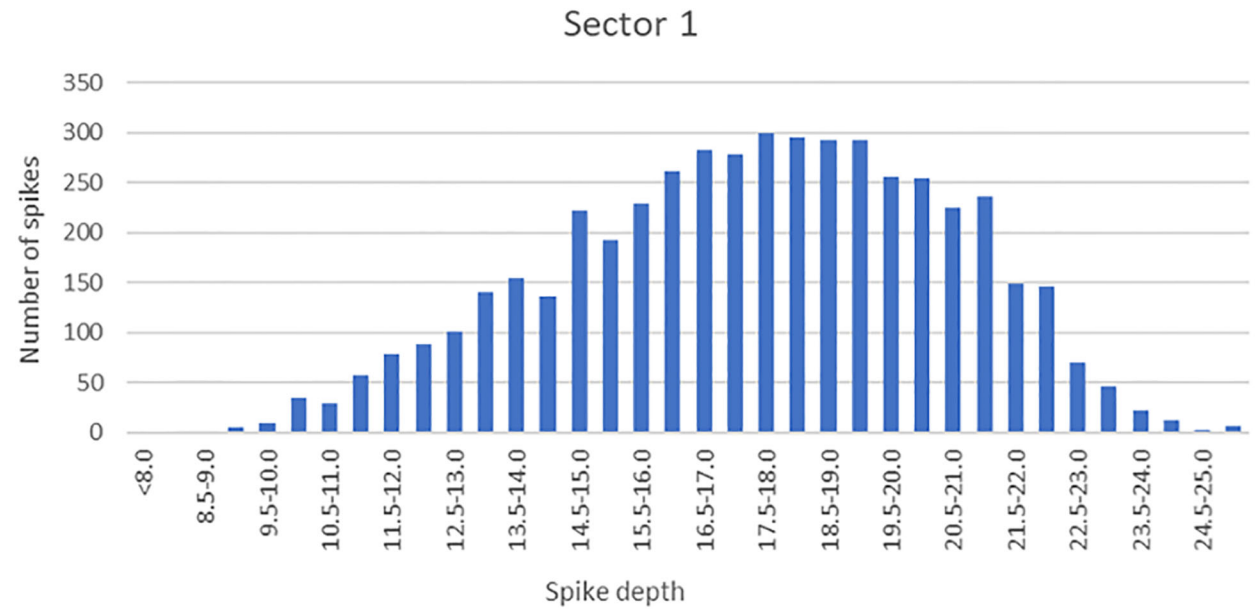

CHART 1
Statistical analysis on the number of spikes relative to the spikes depth for Sector 1.

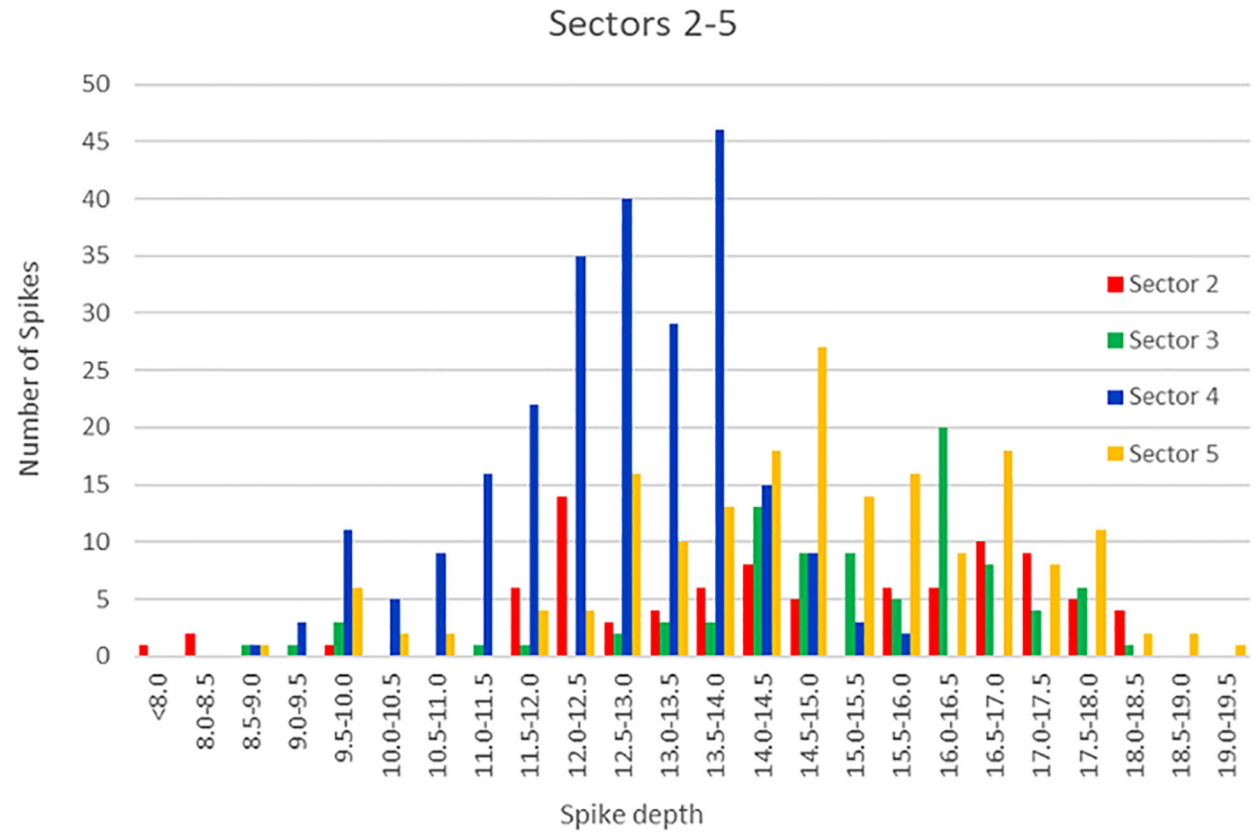

CHART 2
Statistical analysis on the number of spikes relative to the spikes depth for Sectors 2 to 5.

10.3389/fmars.2024.1414673

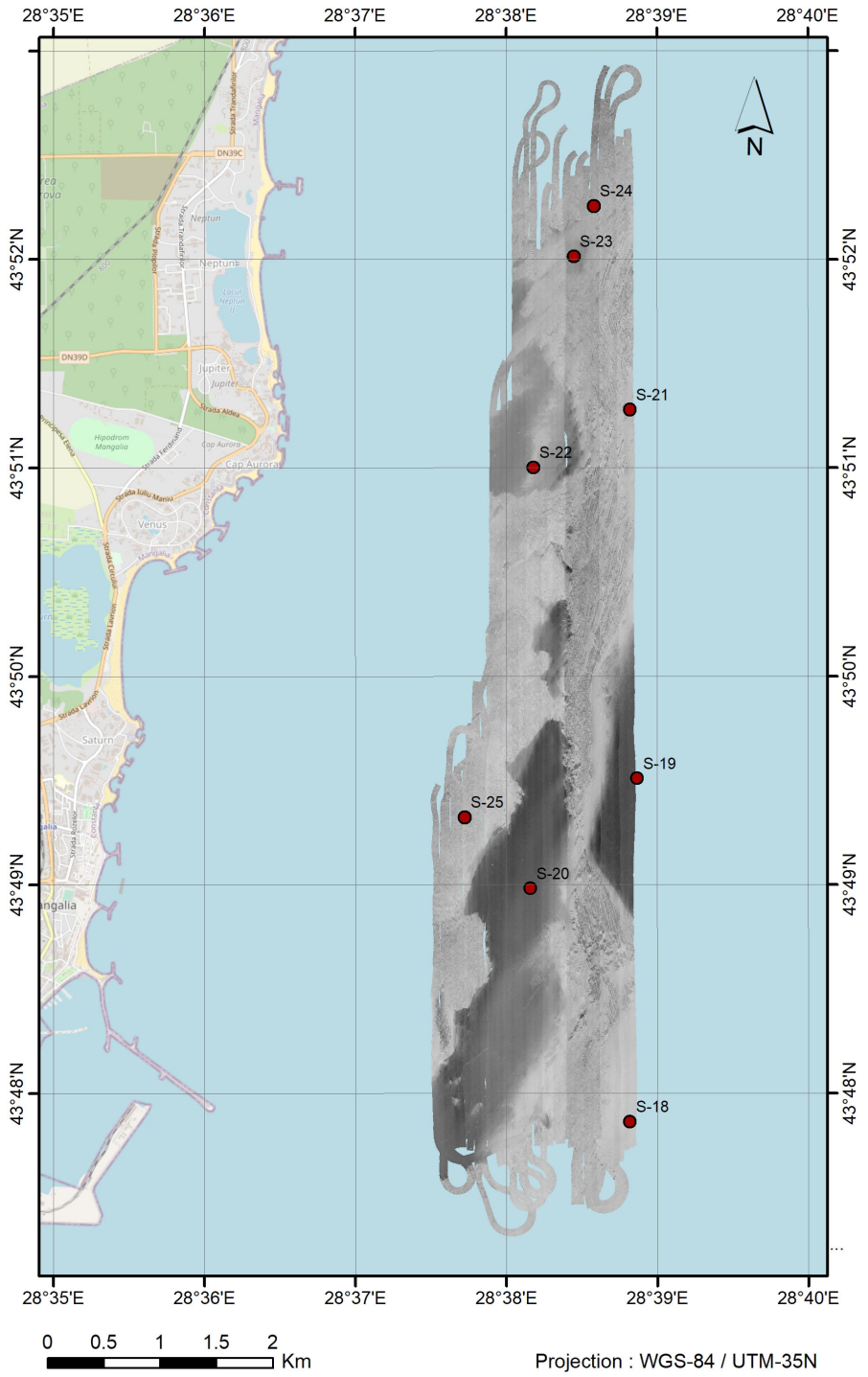

FIGURE 13
Backscatter mosaic of area MN-227-A-02 and sediment sampling stations (marked with red dots).

within an area without any visible seeps in multibeam data. The high concentration of CH_4 in this area can be related to seeps with high gas concentrations in dissolved form, but with no gasses in the form of bubbles that can be detected by MBES measurements.

Although the spatial variability of CH_4 is distinct and related to the seeps, on the distribution map a plume-like extension was recorded with a decreasing gradient toward the western part of the study area (Figure 15). The concentration values in this plume range between 15 and 39 nmol/L, the decreasing gradient corresponding to the intensity of the hotspots. The extension direction of the plume to the western part of the area is in good concordance with the water current direction of 283 degree related

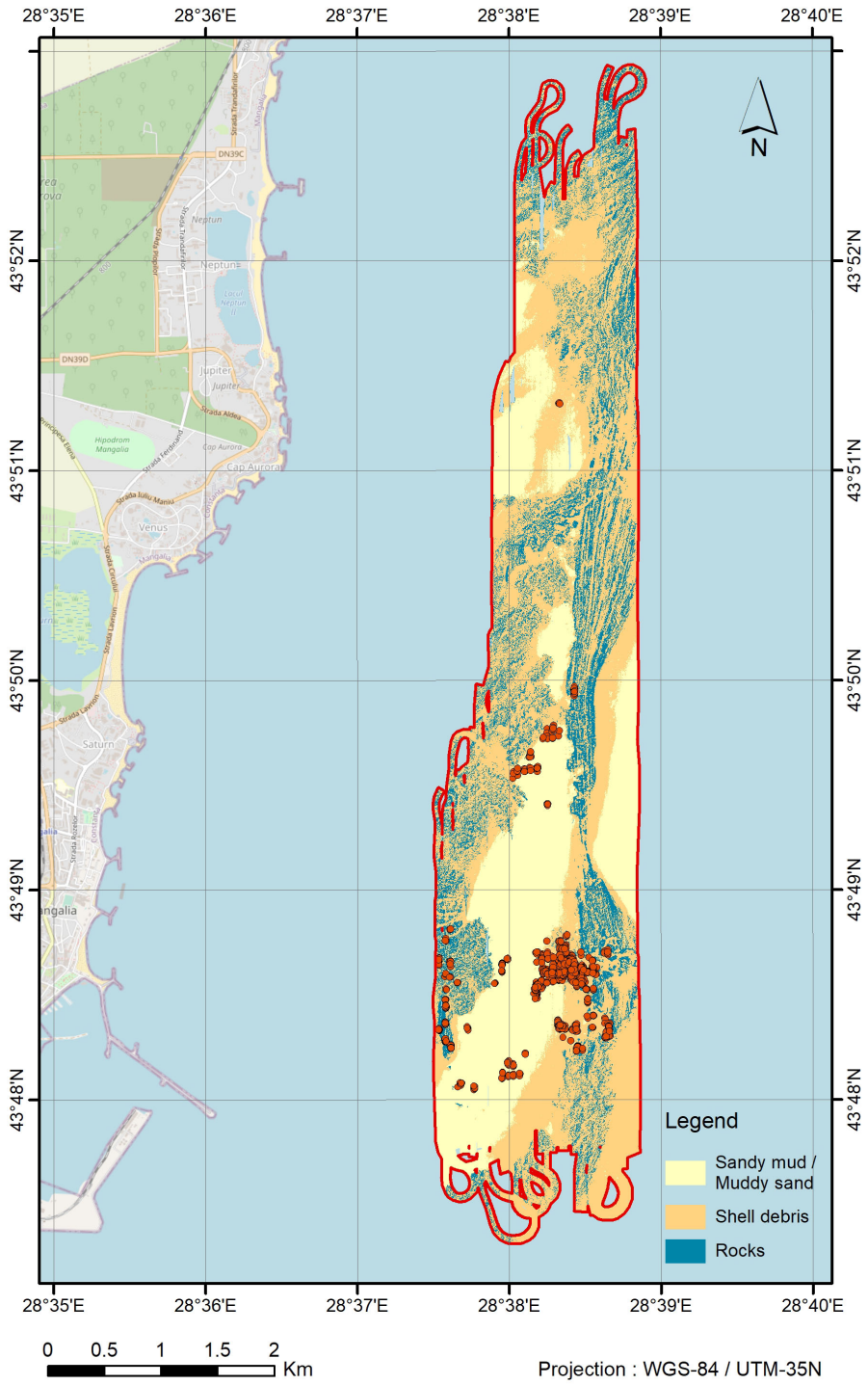

FIGURE 14
Sediment cover of the area MN-227-A-02; with red dots are marked the fluid seeps recorded with the multibeam echosounder.

to North, recorded at the "MEDA" monitoring platform operated by GeoEcoMar in Mangalia Bay, close to the study area. The north-south apparent orientation can be related to the water current orientation on the same direction. The lack of increased concentration of CH_4 in the areas where seeps were detected with geophysical methods may be due to the dispersal of gas in the water column.

The CH_4 has a slightly increased concentration in the second and third sectors, referred to background values (8.5-9 nmol/L), with recorded values between 9.5-12.5 nmol/L. In the fourth sector (in the south-western part of the study area) and in the fifth sector (in the center of the study area), no differences in CH_4 concentration were recorded between areas where fluid seeps were detected and the background values.

4.6 Benthic habitats

Seeps occur on both rocky and sedimentary substrates. Several benthic habitats were identified in their proximity, more or less affected by the outflow of the springs. *In situ* observations shown an area with a diameter of up to 1 m directly affected by these unique conditions. Still, the extent of this influence varies, depending on the volume of the outflow. Three habitats were evidenced in the study area:

1. Infralittoral rocks with biogenic reefs of *Mytilaster lineatus* and *Mytilus galloprovincialis*;
2. Infralittoral shelly coarse sand and shell beds with varied infauna;
3. Lower infralittoral sand and muddy sand with *Upogebia pusilla, Micronephthys longicornis, Prionospio maciolekae, Nephtys hombergii* and *Chamelea gallina*.

Few tolerant macrobenthic species were recorded close to the springs. Species such as *Amphibalanus improvisus, Mytilus galloprovincialis* and *Mytilaster lineatus*, also commonly occur in the surrounding benthic habitats. Macrophytes and seagrass canopy (*Zostera noltii*) are unable to thrive under the direct inflow of sulphurous water. Still, they are well-developed in the areas adjacent

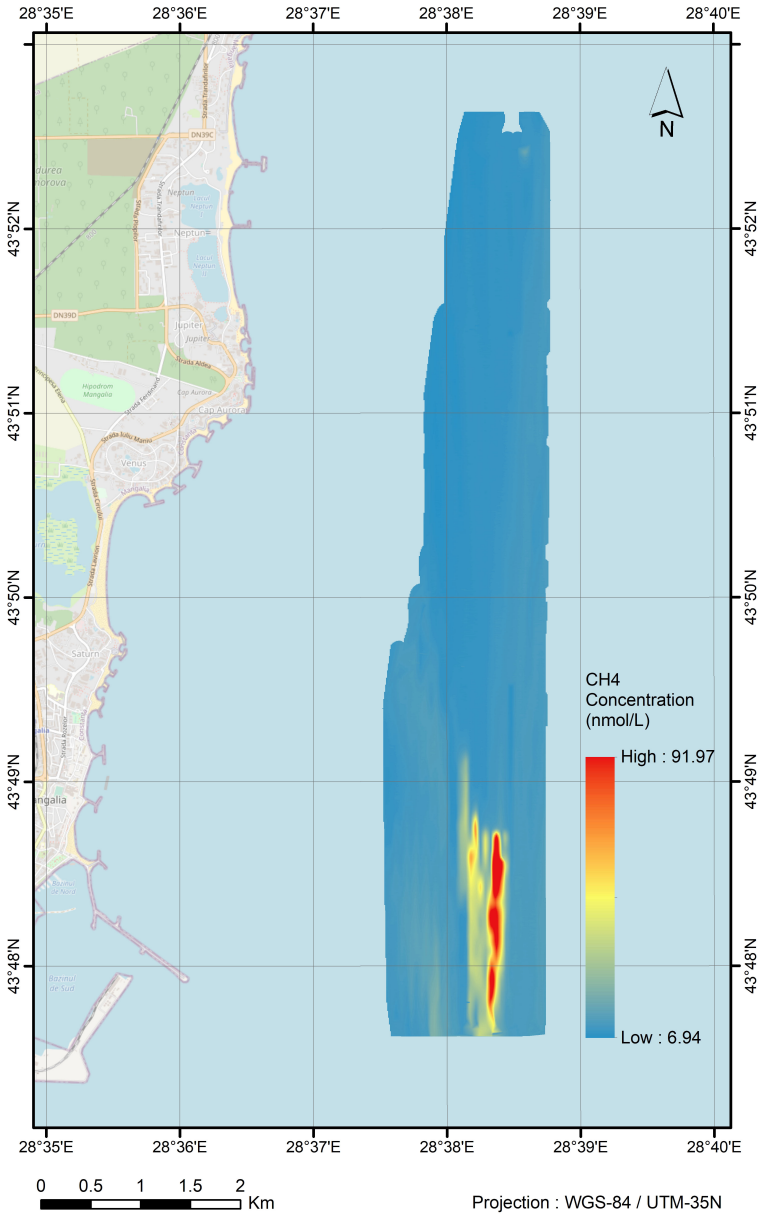

FIGURE 15
CH_4 concentration (in Nmol) measured with Picarro G2301 analyzer in area MN-227-A-02. A consistency/correlation can be observed between the higher CH_4 gas concentration area and the area where the most seeps were detected and recorded (see Figure 13).

to the springs and they support a highly diverse associated fauna, including crustaceans such as amphipods, isopods, and decapods, as well as gastropods (Surugiu et al., 2021).

5 Conclusions

Our extended geological and geophysical surveys on the Romanian Black Sea emphasized Mangalia area as most interesting for underwater sulphurous springs. The sulphurous springs were previously studied, particularly those close to or directly on the shore, and in very shallow waters, indicating a long-standing geological process in Mangalia area. The springs are marked by a distinct white-yellow halo resulting from the sulphur content in the water. During our research cruises, seeps/springs were recorded at greater depths than previously assumed (i.e. no more than 10-15 m), ranging between 22-24 m. These seeps were identified in rocky areas as well as in their vicinity, where the seabed is covered by shell debris or fine sediments.

Multibeam data (bathymetry and water column) coupled with geochemical measurements allowed us to detect the seeps and to pinpoint their location with high accuracy during the two scientific cruises in five sectors. In the first sector, the most active for fluid seeping, the second cruise (MN-240) confirmed the continuity of the fluid seepage after a period of a year and a half. Being detected in the same location in both cruises, we may assume that they have a permanent or at least a semi-permanent flow.

In the whole study area, the majority of the MBES spikes were detected at depths between 14-18 m water depth, with less spikes detected close to the bottom. Few were detected under 14 m and almost no spikes detected less than 10 m below air/water interface. If we exclude an improbable limit detection of the MBES system, this seems to be the limit where the gas is absorbed into the water.

N-S and NE-SW trending faults were interpreted in the area based on sea bottom geology and on bathymetry data collected during the first cruise. Inline positioning of some of the seeping fluids (sectors 2 and 5) also indicate faults even if these could not be detected on the recorded geophysical data. In the first seeping sector, the seabed morphology indicates a doline formed by underground waters circulating in the cracks and faults of carbonate rocks. Fault lines and fractures create pathways for underground fluids, such as sulphurous gases and water, to rise to the surface or seep into the seabed. Limestone and shale beneath the seabed can contribute to the formation of sulphurous springs, as these rocks often contain sulphur-rich minerals that, when exposed to water and pressure, can release sulphurous gases and create underwater sulphurous springs.

There is a good correlation between the occurrence of recorded CH_4 hotspots, above or nearby the underwater springs in sector 1, with the geophysical measurements. In areas with lower seep density (sectors 2-5), they were detected only with geophysical methods. The low correlation of the CRDS gas analyzer data and MBES inferred gas seeps can be explained by the fact the CRDS gas analyzer measure mainly dissolved gasses in water at 1.5 m depth while the MBES gas seeps reflect bubbles of free gas always deeper than 5 m (MBES sensor depth). The methane in lower concentration was absorbed into the sea water before it could be detected by geochemical measurements, as water was sampled from very shallow depth.

The area south of sector 1 show higher concentrations of methane detected with a gas analyzer, while seeps could not be detected with MBES. This fact was attributed to emanations of underground springs without gas bubbles or to a surface water current on a N-S direction. The density map of spikes recorded with the MBES system showed the seeps distribution in the whole area.

The high resolution (20 cm/pixel) physical habitat mosaic obtained and the geomorphological map built based on bathymetry data showed the great diversity of the study area, evidencing rocky areas with the greatest flora and fauna diversity, shell debris covered areas, and fine sediments covered areas where we found evidence of long and continuous seeping activity (pockmarks).

Pockmarks detected in the south of the study area correlate in some cases with active seeps. Although most of the pockmarks did not show seeping activity at the moment of the survey, the inactive pockmarks indicate that fluid seepage was either active in the past or that they have periodic or intermittent fluid seeping. The occurrence of the pockmarks in the whole southern area indicates that the area had intense seeping activity, while in some cases the seepage is still active.

The inventoried seeps as greenhouse gas sources may be further investigated in terms of substrate-to-sea and sea-to-air methane flux.

Being situated in the vicinity of Mangalia city and to other tourist resorts, the study area is prone to human impact due to infrastructure development, fishing, and tourism. Our highly detailed physical habitat map coupled with chemical and biological information, allows better understanding and empowers science-based actions in terms of habitat conservation. Further research will reveal the general changes of the studied area, and will assist the decision-making processes.

Research projects

Proiect Naţional - PN19200302 - Cercetări interdisciplinare privind habitatele bentale şi pelagice de pe platforma românească a Mării Negre în sprijinul dezvoltării/susţinerii sistemelor socio-economice şi a cunoaşterii rolului lor în bioeconomie.

Proiect Naţional – PN23300202 – Dezvoltarea metodelor de abordare ecosistemică a sustenabilităţii resurselor biologice marine (meduze, alge macrofite, moluşte) şi cele de producţie pentru extinderea utilizării biotehnologice a acestora.

Proiect Național - PN23300101 - Gestionarea și monitorizarea mediului marin, parte a strategiei naționale de evidențiere a schimbărilor climatice regionale și globale pe platoul continental românesc al Mării Negre: o analiză complexă pe baza Elaborării hărților geologice, geofizice, biologice și geochimice la scara 1:50.000.

Data availability statement

The raw data supporting the conclusions of this article will be made available by the authors, without undue reservation.

Author contributions

AP: Conceptualization, Data curation, Formal analysis, Investigation, Methodology, Resources, Software, Supervision, Validation, Visualization, Writing – original draft, Writing – review & editing. IMS: Conceptualization, Data curation, Formal analysis, Investigation, Methodology, Resources, Software, Supervision, Validation, Visualization, Writing – original draft, Writing – review & editing. VD: Data curation, Formal analysis, Investigation, Methodology, Resources, Validation, Visualization, Writing – review & editing. AT: Data curation, Formal analysis, Investigation, Methodology, Writing – original draft, Writing – review & editing. SB: Conceptualization, Data curation, Formal analysis, Investigation, Methodology, Resources, Writing – original draft, Writing – review & editing. MEP: Supervision, Writing – review & editing. GI: Data curation, Formal analysis, Investigation, Supervision, Visualization, Writing – review & editing. B-AI: Data curation, Investigation, Methodology, Writing – review & editing.

Funding

The author(s) declare financial support was received for the research, authorship, and/or publication of this article. This study was financially supported by the Romanian Ministry of Research, Innovation and Digitization in the framework of the national CORE Program projects: PN19200302 (Proiect Național - Cercetări interdisciplinare privind habitatele bentale și pelagice de pe platforma românească a Mării Negre în sprijinul dezvoltării/ susținerii sistemelor socio- economice și a cunoașterii rolului lor în bioeconomie), PN23300202 (Proiect Național – Dezvoltarea metodelor de abordare ecosistemică a sustenabilității resurselor biologice marine (meduze, alge macrofite, moluște) și cele de producție pentru extinderea utilizării biotehnologice a acestora) and PN23300101 (Gestionarea și monitorizarea mediului marin, parte a strategiei naționale de evidențiere a schimbărilor climatice regionale și globale pe platoul continental românesc al Mării Negre: o analiză complexă pe baza Elaborării hărților geologice, geofizice, biologice și geochimice la scara 1:50.000). VD was supported by a grant of the Romanian Ministry of Education and Research, CNCS - UEFISCDI, project number PN-III-P4-ID-PCE2020-2282 (ECHOES).

Acknowledgments

We thank all our colleagues who helped us with data recording and processing and who gave us feedbacks and made valuable suggestions on the manuscript. Data recorded during the second cruise (MN-240) were obtained through the project H2020 DOORS (GA no. 101000518), funded by the European Commission. Data recorded at"MEDA" monitoring platform operated by GeoEcoMar in the Mangalia Bay were obtained through the EMSO-EUXINUS project.

Conflict of interest

The authors declare that the research was conducted in the absence of any commercial or financial relationships that could be construed as a potential conflict of interest.

Publisher's note

References

Begun, T., Teacă, A., Muresan, M., Quijón, P. A., Menabit, S., and Surugiu, V. (2022). Habitat and Macrozoobenthic Diversity in Marine Protected Areas of the Southern Romanian Black Sea Coast. *Front. Mar. Sci.* 9. doi: 10.3389/fmars.2022.845507

Begun, T., Teacă, A., Muresan, M., Vasiliu, D., Secrieru, D., and Pavel, B. (2018). Environmental assessment of two MPAs from the Romanian Black Sea Coast. *J. Environ. Prot. Ecol.* 19, 573–582.

Benderev, A., Hristov, V., Bojadgieva, K., and Mihailova, B. (2016). "Thermal waters in Bulgaria," in *Mineral and Thermal Waters of Southeastern Europe, Environmental Earth Sciences*. Ed. P. Papić (Springer International Publishing, Switzerland), 47–64. doi: 10.1007/978-3-319-25379-4_3

Blott, S. J., and Pye, K. (2001). GRADISTAT: a grain size distribution and statistics package for the analysis of unconsolidated sediments. *Earth Surface Processes Landforms* 26, 1237–1248. doi: 10.1002/esp.261

Borges, A., Champenois, W., Gypens, N., Delille, B., and Harlay, J. (2016). Massive marine methane emissions from near-shore shallow coastal areas. *Sci. Rep.* 6, 27908. doi: 10.1038/srep27908

Brad, T., Iepure, S., and Sârbu, Ş. M. (2021). The chemoautotrophically based movile cave groundwater ecosystem, a hotspot of subterranean biodiversity. *Diversity* 13, 128. doi: 10.3390/d13030128

Breier, A. (1976). *Lacurile de pe litoralul românesc al Mării Negre – Studiu hidrogeografic* (Bucharest: Editura Academiei R.S.R.).

Briceag, A., Macaleț, R., and Melinte-Dobrinescu, M. (2018). "Sarmatian paleoenvironment and biovents in the Dobrogea Region (SE Romania)," in *Geo-Eco-Marina, 24/2018* (Bucharest: GeoEcoMar), 81–92. doi: 10.5281/zenodo.2549908

Capotă, A. (1980). *Studiu geologic, hidrologic și chimic privind apele mezotermale sulfuroase din zona Mangalia de Nord* (Bucharest).

Ciocârdel, R., and Protopopescu-Pache, E. (1955). "Considerații hidrogeologice asupra Dobrogei," in *Studii Tehnice și Economice*. Seria E, Nr. 3. (Bucharest: Institutul Geologic al Romaniei).

Clark, J. F., Washburn, L., Hornafius, J. S., and Luyendyk, B. P. (2000). Dissolved hydrocarbon flux from natural marine seeps to the southern California Bight. *J. Geophys. Res.* 105, 11,509–11,522. doi: 10.1029/2000JC000259

Constantinescu, T. (2002). Le Karst de la Zone Mangalia. *Trav. Inst. Speol. Emile Racovitza* XLI-XLII, 89–109.

Cynar, F. J., and Yayanos, A. A. (1992). Distribution of methane in the upper waters of Southern California Bight. *J. Geophys. Res.* 97, 11269–11285. doi: 10.1029/92JC00865

Deike, G. H. (1989). Fracture Controls on Conduit Development. In W. B. White and E. L. White (Eds.) *Karst Hydrology Concepts from the Mammoth Cave Area*. (New York: Springer), 259–291.

Diaconescu, M. (2017). Sisteme de fracturi active crustale pe teritoriul României. Bucharest, Romania: Doctoral School of Geology, Faculty of Geology and Geophysics, University of Bucharest Library Repository. PhD Thesis.

Diaconescu, M., Craiu, A., Toma-Dănilă, D., Craiu, G. M., and Ghiţă, C. (2019). "Main active faults from the eastern part of Romania (Dobrogea and Black Sea)," in *Part I: Longitudinal Faults System, Romanian Reports in Physics* (Bucharest: Editura Academiei Române), vol. 71, 702.

Dimitrov, L. I. (2002a). Mud volcanoes – the most important pathway for degassing deeply buried sediments. *Earth-Sci. Rev.* 59, 49–76. doi: 10.1016/S0012-8252(02)00069-7

Dimitrov, L. (2002b). Contribution to atmospheric methane by natural seepages on the Bulgarian continental shelf. *Continental Shelf Res.* 22, 2429–2442. doi: 10.1016/S0278-4343(02)00055-9

Dinu, C., Wong, H. K., Ţambrea, D., and Maţenco, L. (2005). Stratigraphic and structural characteristics of the Romanian Black Sea shelf. *Tectonophysics* 410, 417–435. doi: 10.1016/j.tecto.2005.04.012

Dragomirescu, C. (1927). *Cercetări hidrogeologice prin foraje executate în Dobrogea de sud* (Bucureşti).

Drăguşin, V., Tîrlă, L., Covaliov, S., Cruceru, N., Mirea, I. C., and Şandric, I. (2021). The unique topography from Obanul Mare (Mangalia, SE Romania): remnant of a maze cave. *Géomorphologie: relief processus environnement* 27, 221–229. doi: 10.4000/geomorphologie.15794

Drăguşin, V., Vlaicu, M., Balan, S. V., Baciu, M., Pop, M. M., and Sambro, O. (2023). Characteristics of submerged and partially submerged caves (habitat type 8330) in Romania. *Environ. Monit. Assess.* 195, 1520. doi: 10.1007/s10661-023-12137-1

Etiope, G., and Klusman, R. W. (2002). Geologic emissions of methane to the atmosphere. *Chemosphere* 49, 777–789. doi: 10.1016/S0045-6535(02)00380-6

Etminan, M., Myhre, G., Highwood, E. J., and Shine, K. P. (2016). Radiative forcing of carbon dioxide, methane, and nitrous oxide: a significant revision of the methane radiative forcing. *Geophys. Res. Lett.* 43, 12614–12623. doi: 10.1002/2016GL071930

Finetti, I., Bricchi, G., Del Ben, A., Pipan, M., and Xuan, Z. (1988). Geophysical study of the Black Sea. *Boll. Geofis. Teor. Appl.* 30, 197–324.

Folk, R. L. (1954). The distinction between grain size and mineral composition in sedimentary rocks. *J. Geol.* 62, 344–359. doi: 10.1086/626171

Georgiev, G. (2012). Geology and hydrocarbon systems in the Western Black Sea. *Turkish J. Earth Sci.* 21, 4. doi: 10.3906/yer-1102-4

Hornafius, J. S., Quigley, D., and Luyendyk, B. P. (1999). The world's most spectacular marine hydrocarbon seeps (Coal Oil Point, Santa Barbara Channel, California): Quantification of emissions. *J. Geophys. Res.* 104, 20,703–20,711. doi: 10.1029/1999JC900148

Horoi, V. (1994). The corrosion process in Pestera de la Movile Cave (Southern Dobrudja-Romania). *Theor. Appl. Karstol.* 7, 187–191.

Houghton, J. T., Ding, Y., Griggs, D. J., Noguer, M., van der Linden, P. J., Dai, X., et al. (2001). *Climate Change 2001: The Scientific Basis: Contribution of Working Group I to the Third Assessment Report of the Intergovernmental Panel on Climate Change* (Cambridge: Cambridge University Press, Cambridge, United Kingdom and New York, NY, USA), 881pp.

Ion, J., Iordan, M., Mărunţeanu, M., and Seghedi, A. (2003). Palacogeography of Dobrogea based on lithofacies maps of the Moesian cover. Complex researches in Southern Dobrogea, with special references on the Movile Region (First part). *Trav. Inst. Speol. "Emile Racovitza"* XLI-XLII, 11–38.

Ionescu, D., Siebert, C., Polerecky, L., Munwes, Y. Y., Lott, C., Häusler, S., et al. (2012). Microbial and chemical characterization of underwater fresh water springs in theDead Sea. *PloS One* 7, e38319. doi: 10.1371/journal.pone.0038319

Ionesi, L. (1994). *Geografia unităţilor de platformă şi a Orogenului Nord-Dobrogean* (Bucharest: Editura Tehnică).

Judd, A. G., Davies, G., Wilson, J., Holmes, R., Baron, G., and Bryden, I. (1997). Contributions to atmospheric methane by natural seepages on the UK continental shelf. *Mar. Geol.* 137, 427–455. doi: 10.1016/S0025-3227(97)00067-4

Judd, A., and Hovland, M. (2007). *Seabed Fluid Flow: The Impact of geology, biology and the marine environment* (Cambridge: Cambridge University Press). doi: 10.1017/CBO9780511535918

Kinkaid, T. (2020). *Search for Submarine Springs & Caves in the Black Sea - 2020* (Reno: Geohydros), 33.

Klusman, R. W., Leopold, M. E., and LeRoy, M. P. (2000). Seasonal variation in methane fluxes from sedimentary basins to the atmosphere: Results from chamber measurements and modeling of transport from deep sources. *J. Geophys. Res.* 105, 24,661–24,670. doi: 10.1029/2000JD900407

Kopf, A. J. (2002). Significance of mud volcanism. *Rev. Geophys.* 40, 1005. doi: 10.1029/2000RG000093

Krautner, H. G., Mureşan, M., and Seghedi, A. (1988). "Precambrian of Dobrogea," in *Precambrian in younger fold belts*. Ed. V. Zoubek (John Wiley, New York), 361–379.

Lan, X., Thoning, K. W., and Dlugokencky, E. J. (2023). *Trends in globally-averaged CH_4 N_2O, and SF_6 determined from NOAA Global Monitoring Laboratory measurements, Version 2023-04* (NOAA Earth System Research Laboratories Global Monitoring Laboratory). doi: 10.15138/P8XG-AA10

Lascu, C., Popa, R., and Sârbu, Ş. (1995). Le karst de Movile (Dobrogea du Sud). *Rev. Roum. Geogr.* 38, 86–93.

Lohrberg, A., Schmale, O., Ostrovsky, I., Niemann, H., Held, P., and Schneider von Deimling, J. (2020). Discovery and quantification of a widespread methane ebullition event in a coastal inlet (Baltic Sea) using a novel sonar strategy. *Sci. Rep.* 10, 4393. doi: 10.1038/s41598-020-60283-0

Major, C. O., Goldstein, S. L., Ryan, W. B. F., Lericolais, G., Piotrowski, A. M., and Hajdas, I. (2006). The co-evolution of Black Sea level and composition through the last deglaciation and its paleoclimate significance. *Quaternary Sci. Rev.* 25, 2031–2047. doi: 10.1016/j.quascirev.2006.01.032

Manga, M. (2001). Using springs to study groundwater flow and active geologic processes. *Annu. Rev. Earth Planet Sci.* 29, 201–228. doi: 10.1146/annurev.earth.29.1.201

Mau, S., Valentine, D. L., Clark, J. F., Reed, J., Camilli, R., and Washburn, L. (2007). Dissolved methane distributions and air-sea flux in the plume of a massive seep field, Coal Oil Point, California. *Geophysical Res. Lett.* 34, L22603. doi: 10.1029/2007GL031344

Munteanu, I. (2012). Evolution of the western Black Sea: Kinematic and sedimentological inferences from geological observations and analogue modelling. Utrecht Studies in Earth Sciences. (Utrecht, Netherlands: Utrecht University). Available at: https://dspace.library.uu.nl/handle/1874/250487. Dissertation.

Oaie, G., Seghedi, A., and Rădulescu, V. (2016). "Natural marine hazards in the Black Sea and the system of their monitoring and real-time warning," in *Geo-Eco-Marina 22/2016* (Bucharest: GeoEcoMar), 5–28. doi: 10.5281/zenodo.889593

Oczlon, M. S., Seghedi, A., and Carrigan, C. W. (2007). "Avalonian and Baltican terranes in the Moesian Platform (southern Europe, Romania, and Bulgaria) in the context of Caledonian terranes along the southwestern margin of the East European craton," in *The evolution of the Rheic Ocean: From Avalonian-Cadomian active margin to Alleghenian-Variscan collision*. Eds. U. Linnemann, R. D. Nance, P. Kraft and G. Zulauf (Geological Society of America), 375–400. doi: 10.1130/2007.2423(18/

Onac, B. P., and Drăguşin, V. (2017). "Hypogene caves of Romania," in *Hypogene Karst Regions and Caves of the World, Cave and Karst Systems of the World*. Eds. A. Klimchouk, A. N. Palmer, J. DeWaele, A. S. Auler and P. Audra (Springer Cham), 257–265. doi: 10.1007/978-3-319-53348-3_16

Öztürk, M. Z., Şener, M. F., Şener, M., and Şimşek, M. (2018). Structural controls on distribution of dolines on Mount Anamas (Taurus Mountains, Turkey). *Geomorphology* 317, 107–116. doi: 10.1016/j.geomorph.2018.05.023

Panin, N. (2005). "The Black Sea coastal zone – an overview," in *Geo-Eco-Marina, 11/2005*, 21–40. doi: 10.5281/zenodo.57388

Panin, N., and Jipa, D. (1998). "Danube river sediment input and its interaction with North-Western Black Sea: results of EROS-2000 and EROS-21 projects," in *Geo-Eco-Marina 3/1998* (Bucharest: GeoEcoMar), 23–35.

Paraschiv, D. (1975). Geologia zăcămintelor de hidrocarburi din România. *Stud. Tehn. Econ. A* 10, 363.

Paraschiv, D. (1979). *Platforma Moesică şi zăcămintele ei de hidrocarburi / The Moesian Platform and its Hydrocarbon Reservoirs* (Bucharest: Editura Academiei Române).

Paraschiv, D. (1983). "Stages in the Moesian Platform history. Lucrările Congresului al XII-lea al Asociaţiei Geologice Carpato-Balcanice - Tectonică, Petrol şi Gaze, Bucharest 1981," in *Anuarul Institutului de Geologie şi Geofizică* (Bucharest: Institutul de Geologie şi Geofizică), vol. 60, 177–188.

Parlichev, D., and Vasilev, A. (2021). New opportunities for identification of precursors of sea earthquakes. *Eng. Geol. Hydrogeol.* 35, 15–22. doi: 10.52321/igh.35.1.15

Pitts, M. W., and Alfaro, C. (2001). "Geologic/hydrogeologic setting and classification of springs," in *Springs and Bottled Waters of the World: ancient History, Source, Occurrence, Quality, and Use*. Eds. P. E. LaMoreaux and J. T. Tanner (Springer-Verlag, Berlin), 34–71.

Pitu, N., Pană, A., and Verioti, A. (2022). Experienţa companiei RAJA S.A în exploatarea acviferelor subterane din Judeţul Constanţa. *Hidrotehnica* 67, 48–58.

Pitu, N., and Verioti, A. (2011). "South Dobrogea underground aquifers and their evolution in the last 40 - 50 years," in *IWA Specialist Groundwater Conference Proceedings*, Belgrad, Serbia.

Popa, I., Mocuţa, M., and Iurkiewicz, A. (2019). "A new regional conceptual model on the hydrogeology of Southern Dobrogea based on seismic surveys and hydro-geological data revisiting," in *Proceedings of 4th IAH CEG Conference*, Donji Milanovac, Serbia.

Popovici, M., and Jianu, L. D. (2006). Mlaştina Hergheliei (Mangalia, jud. Constanţa) – potenţială arie naturală protejată pentru conservarea avifaunistică. *Delta Dunării III Tulcea*, 71–84.

Prescott, J. R., and Habermehl, M. A. (2008). Luminescence dating of spring mound deposits in the Southwestern Great Artesian Basin, Northern South Australia. *Aust. J. Earth Sci.* 55, 167–181. doi: 10.1080/08120090701689340

Romanian Ministry of Health and Institute of Balneology and Physiotherapy (1973). *Apele minerale şi nămolurile terapeutice din R.S.R* Vol. IV (Bucharest: Editura Medicală), 692 p.

Ross, D. A., and Degens, E. T. (1974). "Recent sediments of the Black Sea," in *The Black Sea - Geology, Chemistry and Biology*, vol. 20 . Eds. E. T. Degens and D. A. Ross (AAPG Memoir, Tulsa), 183–199.

Ryan, W. B. F., Pitman, W. C., Major, C. O., Shimkus, K., Moskalenko, V., Jones, G. A., et al. (1997). An abrupt drowning of the Black Sea shelf. *Mar. Geol.* 138, 119–126. doi: 10.1016/S0025-3227(97)00007-8

Sander, R. (2015). Compilation of Henry's law constants (version 4.0) for water as solvent. *Atmospheric Chem. Phys.* 15, 4399–4981. doi: 10.5194/acp-15-4399-2015

Săndulescu, M. (1984). *Geotectonica României* (Bucharest: Editura Tehnică).

Săndulescu, M., and Visarion, M. (2000). Crustal structure and evolution of the Carpathian-Western Black Sea areas. *First Break* 18, 103–108. doi: 10.3997/1365-2397.18.3.26217

Sârbu, M. Ş., Kane, T. C., and Kinkle, B. K. (1996). A chemoautotrophically based cave ecosystem. *Science* 272, 1953–1955. doi: 10.1126/science.272.5270.1953

Sârbu, M. Ş., and Lascu, C. (1997). Condensation corrosion in Movile cave, Romania. *J. Cave Karst Stud.* 59, 99–102.

Sârbu, Ş. M., Lascu, C., and Brad, T. (2019). "Dobrogea: Movile cave," in *Cave and Karst Systems of Romania. Cave and Karst Systems of the World*. Eds. G. M. L. Ponta and B. Onac (Springer, Cham). doi: 10.1007/978-3-319-90747-5_48

Schubert, M., Knöller, K., Stollberg, R., Mallast, U., Ruzsa, G., and Melikadze, G. (2017). Evidence for submarine groundwater discharge into the Black Sea - investigation of two dissimilar geographical settings. *Water* 9, 468. doi: 10.3390/w9070468

Seghedi, A., Berza, T., Iancu, V., Mărunţiu, M., and Oaie, G. (2005a). Neoproterozoic terranes in the Moesian basement and in the Alpine Danubian nappes of the South Carpathians. *Geologica Belgica* 8/4, 4–19.

Seghedi, A., Vaida, M., Iordan, M., and Verniers, J. (2005b). Paleozoic evolution of the Romanian part of the Moesian platform: an overview. *Geologica Belgica* 8/4, 99–120.

Slăvoacă, D., Feru, M., Geamănu, V., Simion, G., Goliţă, N., and Lungu., P. (1978). "Consideraţii hidrogeologice asupra ivirilor de ape termale din România," in *Studii Tehnice şi Economice* (Bucharest: Studii de Hidrogeologie, Institutul Geologic al României), 5–13. Seria E, Nr. 13.

Stanciu, I. M. (2020). Intramoesian fault: geophysical detection and regional active (Neo)Tectonics and geodynamics. Doctoral School of Geology, Faculty of Geology and Geophysics, University of Bucharest Library Repository. PhD Thesis. (Bucharest, Romania: University of Bucharest).

Stanciu, I. M., and Ioane, D. (2021a). "The Moesian platform: structural and tectonic features interpreted on regional gravity and magnetic data," in *Geo-Eco-Marina 27/2021* (Bucharest: GeoEcoMar), 183–195. doi: 10.5281/zenodo.5795188

Stanciu, I. M., and Ioane, D. (2021b). Active fault systems in the Shabla Region (Bulgaria) as interpreted on geophysical and seismicity data. *Rev. Roumaine Geophysique/Romanian Geophysical J.* 63-64/2019-2020, 3–21. doi: 10.5281/zenodo.4543084

Surugiu, V., Teacă, A., Şvedu, I., and Quijón, P. A. (2021). A hotspot in the Romanian Black Sea: eelgrass beds drive local biodiversity in surrounding bare sediments. *Front. Mar. Sci.* 8. doi: 10.3389/fmars.2021.745137

Tari, G., Dicea, O., Faulkerson, J., Georgiev, G., Popov, S., Ştefănescu, M., et al. (1997). "Cimmerian and Alpine stratigraphy and structural evolution of the Moesian Platform," in *Regional and Petroleum Geology of the Black Sea and Surrounding Regions*, vol. 68 . Ed. A. G. Robinson (AAPG Memoir), 63–90.

Tasianas, A., Bünz, S., Bellwald, B., Hammer, Ø., Planke, S., Lebedeva-Ivanova, N., et al. (2018). High-resolution 3D seismic study of pockmarks and shallow fluid flow systems at the Snøhvit hydrocarbon field in the SW Barents Sea. *Mar. Geol.* 403, 247–261. doi: 10.1016/j.margeo.2018.06.012

Tătărâm, N., Rado, G., Pană, I., Hanganu, E., and Grigorescu, D. (1977). "Dobrogea de sud în Neozoic: biostratigrafie şi paleogeografie," in *Studii şi cercetări geologice, geofizice şi geografice* (Bucharest: Editura Academiei R.S.R.), 27–38.

Teacă, A., Begun, T., and Gomoiu, M.-T. (2006). "Recent data on benthic populations from hard bottom mussel community in the Romanian Black Sea coastal zone," in *Geo-Eco-Marina 12/2006* (Bucharest: GeoEcoMar), 43–51.

Teacă, A., Mureşan, M., Menabit, S., Bucse, A., and Begun, T. (2020). Assessment of Romanian circalittoral soft bottom benthic habitats under Danube River influence. *Reg. Stud. Mar. Sci.* 40, 101523. doi: 10.1016/j.rsma.2020.101523

Teleki, N., Munteanu, L., Teodoreanu, E., and Grigore, L. (1984). *Cura Balneoclimatică în România* (Bucharest: Editura Sport-Turism), 351 p.

Udden, J. A. (1914). Mechanical composition of clastic sediments. *Geological Soc. America Bull.* 25, 655–744. doi: 10.1130/GSAB-25-655

Ungureanu, G. V., Lazăr, A. V., Lazăr, R., Balahură, A. D., Ionescu, A. D., Micu, D., et al. (2015). Technical Note - Habitat mapping of Romanian Natura 2000 sites. A case study, "Underwater Sulfurous Seeps, Mangalia". *Ital. J. Geosci.* 134, 69–73. doi: 10.3301/IJG.2014.57

Vasilev, A., Tsekov, M., Petsinski, P., Gerilowski, K., Slabakova, V., Trukhchev, D., et al. (2021). New possible earthquake precursor and initial area for satellite monitoring. *Front. Earth Sci.* 8. doi: 10.3389/feart.2020.586283

Visarion, M., Maier, O., Nedelcu-Ion, C., and Alexandrescu, R. (1979). "Modelul structural al metamorfitelor de la Palazu Mare, rezultat din studiul integrat al datelor geologie, geofizice şi petrofizice," in *Studii şi cercetări de Geologie, Geofizică şi Geografie* (Bucharest: Editura Academiei R.S.R.), vol. 17, 95–113.

Visarion, M., Săndulescu, M., Roşca, V., Stănică, D., and Atanasiu, L. (1990). La Dobrogea dans le cadre de l'avant–pays Carpatique. *Rev. Roum. Geophysique* 34, 55–65.

Visarion, M., Săndulescu, M., Stănică, D., and Veliciu, S. (1988). Contributions à la connaissance de la structure profonde de la plateforme Moésienne en Roumanie. *Stud. Teh. Econ.-Geofiz.* 15, 68–92.

Ward, B. B. (1992). The subsurface methane maximum in the California Bight. *Cont. Shelf Res.* 12, 735–752. doi: 10.1016/0278-4343(92)90028-I

Weber, T., Wiseman, N. A., and Kock, A. (2019). Global ocean methane emissions dominated by shallow coastal waters. *Nat. Commun.* 10, 1–10. doi: 10.1038/s41467-019-12541-7

Wentworth, C. K. (1922). A scale of grade and class terms for clastic sediments. *J. Geol.* 30, 377–392. doi: 10.1086/622910

Williams, P. W. (1972). Morphometric analysis of polygonal karst in New Guinea. *Geological Soc. America Bull.* 83, 761–796. doi: 10.1130/0016-7606(1972)83[761:MAOPKI]2.0.CO;2

Zaharia, T., Anton, E., and Radu, G. (2013). *Ghid sintetic de monitorizare pentru speciile marine şi habitatele costiere şi marine de interes comunitar din România* (Constanţa: Editura Boldaş), 149 p.

Zaharia, T., Micu, D., Nita, V., Maximov, V., Mateescu, R., Spinu, A., et al. (2012). Preliminary data on habitat mapping in the Romanian natura 2000 marine sites. *J. Environ. Prot. Ecol.* 13, 1776–1782.

Zamfirescu, F., Danchiv, A., Popa, I., Popa, R., and Rudolph-Lund, K. (2010). "Chapter 3.17. Southern Dobrogea," in *Karst Hydrogeology of Romania*. Eds. I. Orăşeanu and A. Iurkiewicz (Belvedere Publishing House, Oradea), 351–360.

Zamfirescu, F., Moldoveanu, V., Dinu, C., Pitu, N., Albu, M., Danchiv, A., et al. (1994). "Vulnerability to pollution of karst aquifer system in Southern Dobrogea," in *Proceedings of the International Hydrogeological Symposium on Impact of Industrial Activities on Groundwater*. 591–602.

Zektser, I. S., Everett, L. G., and Dzhamalov, R. G. (2006). *Submarine Groundwater. 1st ed* (Boca Raton: CRC Press). doi: 10.1201/9781420005257